

GASEOUS TRANSPORT IN THE VADOSE ZONE:
COMPUTER SIMULATIONS USING THE DISCRETE STATE COMPARTMENT MODEL

by

Rick Hugh Seidemann

A Thesis Submitted to the Faculty of the
DEPARTMENT OF HYDROLOGY AND WATER RESOURCES
In Partial Fulfillment of the Requirements
For the Degree of

MASTER OF SCIENCE
WITH A MAJOR IN HYDROLOGY

In the Graduate College
THE UNIVERSITY OF ARIZONA

1988

STATEMENT BY AUTHOR

This masters thesis has been submitted in partial fulfillment of requirements for an advanced degree at The University of Arizona and is deposited in the University Library to be made available to borrowers under rules of the Library.

Quotations from this thesis are allowable without special permission, provided that accurate acknowledgement of source is made. Requests for permission for extended quotation from or reproduction of this manuscript in whole or in part may be granted by the head of the major department of the Dean of the Graduate College when in his or her judgement the proposed use of the material is in the interests of scholarship. In all other instances, however, permission must be obtained from the author.

SIGNED: *Rick Seidemann*

APPROVAL BY THESIS DIRECTOR

This thesis has been approved on the date shown below:

Eugene S. Simpson
Eugene S. Simpson
Professor Emeritus of
Hydrology and Water Resources

29 Apr. 88
Date

DEDICATION

Up, down and all around water may flow,
but if you seek your special self its' to New Zealand you must go,

Yeah, Ingrid.

ACKNOWLEDGEMENTS

I would like to thank Dr. Eugene Simpson for his enormous effort in helping me complete my thesis. I would also like to thank my other thesis advisors, Dr. Daniel Evans and Dr. Harold Bently.

Along the way there were a great many other people who helped me complete my degree including Eva and George Starbuck, Dave Kreamer, Toolie, the Slimy Scammer, Da od, Don Don, Vern and Buffy, Number 9, Ron Green, Todd Rasmussen and many other great people in the Hydro Department and at HGC. I thank you all.

TABLE OF CONTENTS

	<u>Page</u>
LIST OF FIGURES	vii
LIST OF TABLES	ix
ABSTRACT	xi
1. INTRODUCTION	1
Problem Definition	1
Background	2
Data Collection and Analysis	6
2. TRANSPORT OF TCE IN THE VADOSE ZONE	9
Introduction	9
Molecular Diffusion and the Effective	
Diffusion Coefficient	9
Advective Gaseous Flow	13
Advection of Soil Water	14
Distribution of TCE between the Gas, Liquid, and	
Solid Phases	16
Relative Importance of Parameters	18
Molecular Gaseous Diffusion	18
Effective Diffusion Coefficient	19
Apparent Diffusion Coefficient	22
Advective Gaseous Flow	24
Advection of Water	27
3. DISCRETE-STATE COMPARTMENT MODEL	29
Introduction	29
Operation of the DSC model	30
Advection Subroutine	32
Exchange Subroutine	34
Barometric Subroutine	36
Applications of the DSC Model	36
Analytical Solution	37
Model Parameter Formulation	45
The Compartmental System	45
The Time Step	45
Initial Cell State	45
System Boundary Recharge Concentration	46
Exchange Factor	47
Equivalent Volume of the Compartment	47

TABLE OF CONTENTS (Continued)

	<u>Page</u>
4. SIMULATION STUDIES	50
Introduction	50
Scenario 1a and 1b	51
Scenario 2	56
Scenario 3	59
Scenario 4	62
Scenario 5	65
Scenario 6	67
Scenario 7	70
5. DISCUSSION AND SUMMARY	74
LIST OF REFERENCES	80

LIST OF FIGURES

<u>Figure</u>	<u>Page</u>
1.1 Carranza site and it's relationship to the Tucson International Airport and Hughes Aircraft Company	3
1.2 Stratigraphic description and location of gas samplers at the Carranza site	7
2.1 Barometric pressure at the Carranza site after noon on 10-13-84 at land surface (circles), at a depth of 7.5 m (diamonds), at a depth of 11.5 m (squares), and at a depth of 22.5 m (triangles)	26
3.1 Stepwise operation of two advection algorithms by DSC model (Rasmussen, 1982)	33
3.2 Stepwise operation of two exchange algorithms by DSC model (Rasmussen, 1982)	35
4.1 Homogenous compartmental system used in scenario 1a. Effective diffusion coefficient = $3.63 \text{ E-}3 \text{ m}^2/\text{day}$	52
4.2 TCE concentration (ug/l) profile of scenario 1a after 25 years, plus sign, and the measured concentration profile, squares	54
4.3 1-dimensional system used in scenario 2 with the apparent diffusion coefficient, D_a , shown for individual rows	57
4.4 2-dimensional system used in scenario 3, with the apparent diffusion coefficients, D_a , shown for columns 2, 3, 4, and 5 of individual rows. Column 1 represents a high permeable column with $D_a = 2.00 \text{ E-}2$. Circles represent sampling locations	60
4.5 2-dimensional system used in scenario 4, with the apparent diffusion coefficients, D_a , shown for columns 2, 3, 4, and 5 of individual rows. Column 1 represents a high permeable column with $D_a = 2.00 \text{ E-}2$. Circles represent sampling locations. Compartments with x's in columns 2, 3, and 4 had R_i values changed to represent horizontal heterogeneities as listed in Table 4.6	63

LIST OF FIGURES (Continued)

<u>Figure</u>		<u>Page</u>
4.6	2-dimensional system used in scenario 5 with the apparent diffusion coefficients, D_a , shown for individual rows and location of system boundary recharge concentrations (SBRC) used to simulate lateral diffusion	66
4.7	1-dimensional compartment system of scenario 6 used to simulate gaseous diffusion and barometric pressure fluctuations causing gaseous advection and dispersion . . .	68
4.8	Concentration profile of scenario 6b, triangles, after 25 years and the measured concentration profile, squares . . .	71
4.9	Concentration profile of scenario 7 after 25 years. Without advection, plus sign, with advection, diamonds, and the measured concentrations, squares	73

LIST OF TABLES

<u>Table</u>	<u>Page</u>	
1.1	Vertical distribution of TCE in the soil gas of the vadose zone for different studies. All concentrations are in ug/l. WT is the depth of the water table	5
2.1	Partial list of published expressions relating tortuosity to air-filled (n_a) and total porosity (n) of medium (Weeks et al., 1982)	12
2.2	Some properties of TCE	16
2.3	Air/soil distribution coefficient (K_S) for TCE measured over varying degrees of saturation (Marrin, 1984)	18
2.4	Average temperatures and standard deviations measured at the Carranza site at depths of the gas sampling apparatus during the months of August and September, 1984. Listed temperatures are averages of 23 samples	19
2.5	Grain size distribution for different depths at the Carranza site	21
2.6	Values of water content (W_C), porosity (n), air-filled porosity (n_a), degree of saturation (S), air/soil distribution coefficient (K_S), and effective diffusion coefficient (D_e)	23
3.1	Comparison of the DSC model and the analytic solution, $\Delta t =$ one week	40
3.2	Comparison of the DSC model and the analytic solution, $\Delta x = 27.7$ cm	41
3.3	Comparison of the different mixing algorithms of the DSC model for $\Delta x = 27.7$ cm, $\Delta t = 1$ week, and $Ri = 0.788$	42
3.4	Comparison of the different mixing algorithms of the DSC model for $\Delta x = 249$ cm, $\Delta t = 1$ week, and $Ri = 0.00975$	43
3.5	Comparison of the DSC model using the SMC and the analytic solution, $\Delta x = 27.7$ cm and $\Delta t = 1$ day, with the difference and percentage error	44

LIST OF TABLES (Continued)

<u>Table</u>	<u>Page</u>	
3.6	Concentrations of TCE measured in groundwater in proximity to the Carranza site	46
3.7	Values of volume gas, (Vol_{gas}), volume equivalent, (Vol_{eq}), apparent diffusion coefficient (D_a), and exchange factor (R_i) used in the computer simulations for the different depths	49
4.1	TCE mean concentrations and standard deviations of soil gas samples at the Carranza site at depths of the gas sampling apparatus. The values are based on 23 samples taken from each depth during August and September, 1984	51
4.2	TCE concentration (ug/l) profile of scenario 1a, after 25 years and the measured concentration profile	53
4.3	TCE concentration (ug/l) profile of scenario 1b at different time intervals and the measured concentration profile . . .	56
4.4	TCE concentration (ug/l) profile of scenario 2 at different time intervals and the measured concentration profile . . .	58
4.5	TCE concentration (ug/l) profile of scenario 3 at different time intervals and the measured concentration profile . . .	61
4.6	Rows at which the center three compartments R_i value was changed from scenario 3 to scenario 4 to represent horizontal heterogeneity in the vadose zone	64
4.7	TCE concentration (ug/l) profile of scenario 4 at different time intervals and the measured concentration profile . . .	65
4.8	TCE concentration (ug/l) profile of scenario 5 at different time intervals and the measured concentration profile . . .	67
4.9	Concentrations for scenario 6a, gaseous diffusion in a heterogenous system at different time intervals and the measured concentration profile	69
4.10	Concentrations for scenario 6b, gas diffusion and gas advective transport in a heterogenous system at different time intervals and the measured concentration profile . . .	70
4.11	TCE concentration (ug/l) profile of scenario 7 after 25 years and the measured concentration profile	72

ABSTRACT

Past disposal practices of Trichloroethylene (TCE) and other halogenated hydrocarbons have resulted in the contamination of groundwater in part of the Tucson Basin, Tucson, Arizona. At the Carranza site, known to overlie a TCE groundwater contamination plume, a nest of gas sampling piezometers was constructed to measure the vertical distribution of TCE vapor in the vadose zone. The distribution of TCE vapor in the vadose zone was found to be nonmonotonically decreasing from the water table to the atmosphere. To investigate this TCE concentration profile, simulation studies were performed using the Discrete State Compartment model to test various hypotheses concerning the transport mechanisms of TCE vapor in the vadose zone.

The studies showed that unless a high permeable column by which diffusing gas could by-pass low permeable layers was included in the simulation molecular diffusion alone could not produce the concentrations measured at the Carranza site. The simulation also showed that a nonmonotonic concentration profile similar to the measured concentration profile could be produced if multiple sources are assumed in the vadose zone. Soil gas advection by barometric pressure fluctuations was shown to increase concentrations at all depths in the vadose zone but the effect was minor compared with the effect of the high permeability column by-pass for TCE diffusional transport.

CHAPTER 1

INTRODUCTION

In recent years a growing concern has developed over contamination of groundwater resulting from past discharges of Volatile Organic Compounds (VOCs) into unlined pits and dry wells. Of major concern are halogenated hydrocarbons, such as trichloroethylene (TCE), because of their suspected carcinogenicity. TCE occurs more frequently and at higher concentrations than any other pollutant in the United States groundwater supplies (Dyksen and Hess, 1982). TCE contamination caused the closure of wells in the Tucson Basin by the Tucson Water Department (Montgomery et al., 1984). An evaluation of the vadose zone concentration of TCE associated with the Tucson Basin plume is the subject of this study.

Problem Definition

When sufficient quantities of VOCs are discharged into the vadose zone, downward percolation of the VOC's to the water table can be expected. Once at the water table the VOCs mix with the groundwater and are carried with the groundwater down the hydraulic gradient. This transport mechanism would allow the VOC's to be carried away from the original site of contamination. However, because VOC's have a high vapor pressure, they tend to volatilize out of the groundwater and into the vadose zone, eventually reaching land surface.

In the above scenario the groundwater would be the source of the VOCs in the vadose zone. If the only process transporting the VOCs upward is gaseous diffusion, a monotonically decreasing concentration gradient would occur. This concentration gradient would allow the delineation of contaminant plumes in groundwater by shallow soil gas measurements.

A monotonically decreasing concentration gradient of TCE was not found in this study at the Carranza site or by Marrin (1984), whose study was near the Carranza site. Although the highest concentrations of TCE were found nearest to the water table, the lowest concentrations were not found nearest to land surface. Evidently, the vertical distribution of TCE in the vadose is controlled by more than vertical gaseous diffusion. Other factors need to be considered including lateral diffusion, soil gas advection, soil water distribution and movement, and vertical and horizontal inhomogeneities in the vadose zone.

The objective of this study is to develop insight into the transport mechanisms of TCE in the vadose zone that could produce a nonmonotonic concentration profile. Computer simulations are used to test various hypotheses concerning the transport mechanisms of TCE in the vadose zone. Conclusions reached from the computer simulations will aid understanding, and perhaps predicting, the distribution of VOCs in the soil environment.

BACKGROUND

Recently other soil gas studies have been done that are of direct interest to this study. Marrin (1984) conducted a soil gas study at the Tucson International Airport (Figure 1.1), in Tucson, Arizona, directly

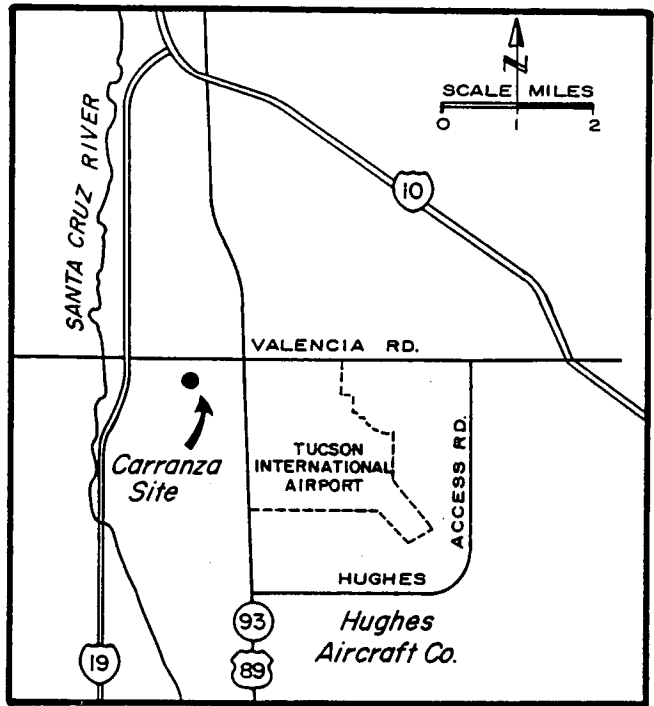


Figure 1.1. Carranza site and it's relationship to the Tucson International Airport and Hughes Aircraft Company.

adjacent to the Hughes Aircraft Company. Shallow soil gas samples (< 2 m deep) were collected from hollow steel probes driven into the soil and then analyzed to determine the relationship between VOC concentration in soil gas of the vadose zone and groundwater. The groundwater samples were obtained from five observation wells. Four vertical borings were drilled to the water table to obtain profiles of the soil gas concentrations, air porosity, and water saturation. Analyses of the VOCs were made on site by a gas chromatograph mounted in a van.

Thomson (1985) also studied the vertical distribution of VOCs in the vadose zone. The study was performed at a well five meters from the Carranza study's gas-sampling piezometer nest. Thomson's vertical boring was drilled with a hollow stem auger. Drilling was interrupted at intermediate depths for soil gas samples to be collected by drive-point screens that were driven or buried in the hole. Analyses of samples was done on site by a gas chromatograph mounted in a van. The vertical boring was not backfilled at completion of the study but was capped.

A comparison of the vertical distribution of TCE concentrations in the soil gas from this and other studies is shown in Table 1.1. The values from Marrin (1984) are higher because of closer proximity to the contamination source. It can be seen that only the Thomson study measured a soil gas concentration profile that decreased monotonically upward.

The study site (Figure 1.1), called the Carranza site after a former owner, is located at 7019 South Sixth Street, Tucson, Arizona. The site is known to overlie a VOC contaminated aquifer. The Carranza site is located 1 kilometer northwest, and down the regional groundwater gradient, from the Hughes Aircraft Company (HAC) near the Tucson Interna-

TABLE 1.1

Vertical distribution of TCE in the soil gas of the vadose zone for different studies. All concentrations are in ug/l. WT is the depth of the water table.

Depth (m)	Carranza study *	Thomson (1985)	Marrin (1984) Boring Number		
			80	175	310
1.5	0.013				
1.8			0.001	0.003	0.120
3.0	0.019	0.006			
7.5	0.005	0.020			
7.7			0.010		
8.0				0.040	0.530
13.5	0.008				
13.8			0.016		
14.2					2.40
15.0		0.090			
17.2				0.098	
20.3			0.012		
21.0	0.575				
26.5			0.012		1.00
27.0		9.00			
30.0	WT	WT			
32.6			0.006		0.220
33.5				WT	
35.7			0.007		
36.2					WT
37.5			WT		

* Concentrations reported are mean values of 23 samples.

tional Airport. From 1951 to 1977 the HAC had been disposing a variety of liquid wastes in pits, lagoons, and trenches. It was determined that TCE and other VOCs were constituents of the wastewater discharged and that these pollutants found their way into both perched water layers and the regional aquifer (Hargis and Montgomery, 1982).

Data Collection and Analysis

To characterize the concentration profile of VOCs in the soil gas at the Carranza site, a vertical nest of air piezometers/gas samplers was constructed. Five permanent samplers were installed in a single auger-drilled borehole at depths 1.5, 3.0, 7.5, 13.5, and 22.0 meters below land surface. Each sample point was surrounded by 20-mesh silica sand and 0.60 m seals of concrete grout were emplaced above each point to prevent vertical movement between the stations. During drilling, soil samples were collected with a split spoon and later analyzed for moisture content, texture, and particle size distribution. Figure 1.2 gives the stratigraphic description and location of samplers.

Gas samples were collected through 0.32 cm stainless steel tubing fitted with a 1.27 cm diameter copper screen at the tip, and a shutoff toggle valve and hose connector at the surface. A peristaltic pump was used to bring the gas sample to land surface. A syringe sample was then taken from the sampling line. The samples were then transported to the University of Arizona, located 15 kilometers north of the study site. After a one- to four-hour period after sample collection, the samples were then injected into a Varian 3700 series gas chromatograph, equipped with an electron capture detector. The column used was a 1/4-inch O.D.

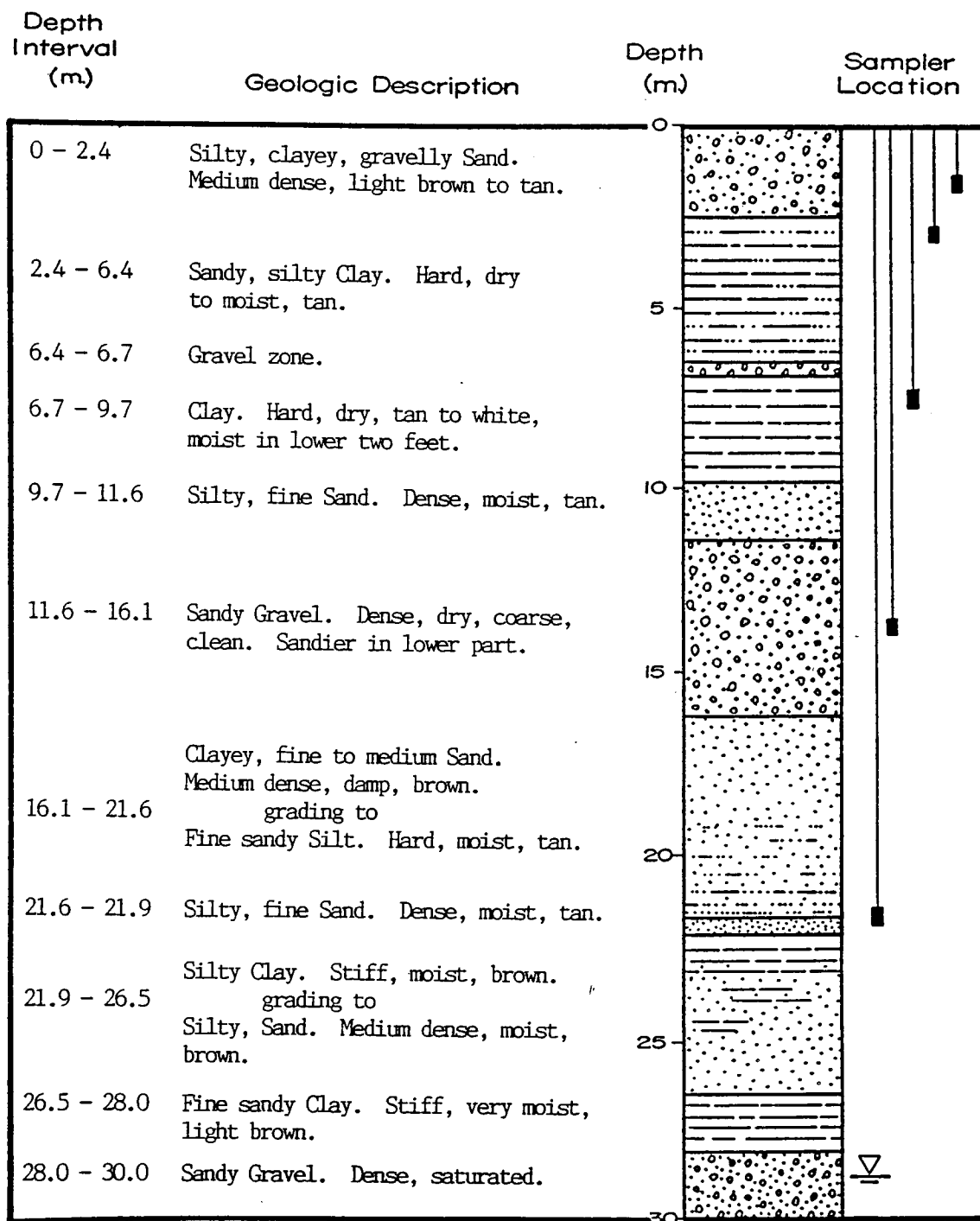


Figure 1.2. Stratigraphic description and location of gas samplers at the Carranza Site.

10-foot, 10% SP2100 on 60/80 mesh Supelcoport. A Nafion desiccant system was used. Standards were run concurrently with gas samples. The halo-carbons analyzed for were: chloroform, carbon tetrachloride, tetrachloroethene, and trichloroethene (TCE).

A relative pressure of subsurface gases was measured in the air piezometer by an inclined manometer, with a sensitivity of 0.25 mm mercury. Each piezometer tip was fitted with a thermistor whose coaxial lead was taped the entire length of the tubing. Temperature was measured over time with a thermistor calibrated to a temperature sensitivity of 0.1 °C. Meteorologic data were obtained from the National Weather Service Station located at the Tucson International Airport.

CHAPTER 2

TRANSPORT OF TCE IN THE VADOSE ZONE

Introduction

Transport of TCE in the vadose zone could occur by many different processes. Transport in the gaseous phase could occur by diffusion or advection of the soil gases. TCE could also be transported as a solute in percolating water. Chemical properties of TCE such as water solubility, critical temperature, molecular weight and size, vapor pressure, coefficient of molecular diffusion, and polarity come into play in determining the magnitude of the mass flux of TCE by each of these transport mechanisms. Also important are properties of the porous medium such as water and organic content, grain size distribution, and porosity. Climatic conditions such as temperature, rainfall, and barometric pressure can also affect the mass flux of TCE. Computer simulations incorporating these factors were made to estimate their relative importance in determining the magnitude of TCE movement at the Carranza site.

Molecular Diffusion and the Effective Diffusion Coefficient

Molecular diffusion is defined as the net flux of a gas from a region of higher concentration to one of a lower concentration resulting only from thermo-kinetic motion of gas molecules. It is analogous to the conductive of heat in solids in response to thermal gradients. Fick

recognized this and adapted the mathematical equations for heat conduction to quantify molecular diffusion (Crank, 1975). Fick's first law of diffusion, in one dimension, states that in an isotropic medium the rate of transfer of the diffusing gas through a unit area of a section is proportional to the concentration gradient measured normal to the section, or

$$F = - D \, dC/dx \quad (2.1)$$

where

F = the mass flux per unit area in the x-direction,

D = coefficient of molecular diffusion,

C = concentration of diffusing gas,

x = direction along which diffusion occurs.

Fick's second law of diffusion incorporates the first law into the continuity equation to obtain in one dimension,

$$\partial C / \partial t = D \, \partial^2 C / \partial x^2 \quad (2.2)$$

where t = time.

In equation 2.1 and 2.2 the coefficient of molecular diffusion, D, is assumed independent of concentration.

The general diffusion coefficient, D_{ab} , describes the diffusion of gas, A, into another gas, B. Slattery and Bird (1958) used simplified kinetic theory and corresponding state arguments to develop an equation for the binary and self diffusion coefficients for non-polar gases into air (Weeks et al., 1982). Even though TCE is slightly polar it will be considered non-polar and its general diffusion coefficient will be calculated from the following equation of Slattery and Bird (1958),

$$D_{ab} = [(P_{ca}P_{cb})^{1/3} (T_{ca}T_{cb})^{5/12} (1/M_a + 1/M_b)^{1/2} / P] * \\ a [T / (T_{ca}T_{cb})^{1/2}]^b \quad (2.3)$$

where

- D_{ab} = general diffusion coefficient (cm²/sec),
 P_c = critical pressure for gas a or b (atm),
 T_c = critical temperature for gas a or b (°K),
 M = molecular weight of designated gas (g/ mole),
 P = prevailing pressure (atm),
 T = prevailing temperature (°K),
 a = 2.745×10^{-4} (a constant),
 b = 1.823 (a constant).

Self diffusion of gases in open vessels and self-diffusion in porous media are different because the tortuosity of paths and changes in cross-sectional area of paths in porous media. A reduction in cross-sectional area will act as an impedance to diffusion. This impedance is often referred to as the tortuosity factor. Equation 2.4 illustrates the relationship between the general diffusion coefficient, D_{ab} , tortuosity factor, β , and the effective diffusion coefficient, D_e . D_e relates to the diffusion of a nonreactive gas through a porous medium.

$$D_e = D_{ab} * \beta \quad (2.4)$$

Many investigators have proposed general relationships between the tortuosity factor and drained and/or total porosity. Weeks et al. (1982) gave a partial list of these relationships which is presented in Table 2.1. They concluded relationships based only on drained and total

TABLE 2.1

Partial list of published expressions relating tortuosity to air-filled (n_a) and total porosity (n) of medium (Weeks et al., 1982).

<u>Investigator</u>	<u>Tortuosity Factor</u>	
	<u>Dry</u>	<u>Wet</u>
Buckingham	n	n_a
Penman	0.66	0.66
van Bavel	0.6	0.6
Marshall	$n_a^{1/2}$	
Millington	$n_a^{4/3}$	$n_a^{4/3}(n_a/n)^2$
Wesseling		$0.9 n_a - 0.1$
Grable and Siemer		$5.25 n_a^{2.36}$
Currie		$n^{1/2} (n_a/n)^4$
de Jong and Schappert		$0.31 - 0.59(n - n_a)$
Lai et al.		$n_a^{4/3}$
Alberston		$0.777 (n_a/n) - 0.274$

porosity were inadequate and that pore geometry, pore size distribution, and the nature of the pore interconnections of the medium must be considered. Only the relationships proposed by Millington and Marshall in Table 2.1 incorporates theoretical pore size distribution models (Weeks et al., 1982).

Weeks et al. (1982) also proposed a relationship between D_{ab} and D_e . It included gas adsorption onto soil particles and absorption of gas into the liquid phase and is,

$$D_e = n_a \beta D_{ab} / [n_a + (n - n_a) \rho_w K_w + \rho_s(1 - n) K_s] \quad (2.5)$$

where

n_a = air porosity,

n = total porosity,

K_w = liquid/gas distribution coefficient,

K_s = gas/liquid/solid distribution coefficient.

Advective Gaseous Flow

Advective flow of gases, also known as forced diffusion, is the movement in response to a gradient of total gas pressure and results in the entire mass of soil gas streaming from a zone of higher pressure to one of lower pressure. Advective flow of gases is similar and dissimilar to the flow of water in porous media. Water is relatively incompressible compared to air, which is highly compressible, so that air's density and viscosity are dependent on pressure and temperature of the system. The similarity is that both air and water flow are impelled by and proportional to a pressure gradient (Hillel, 1980). Hillel (1980) states that it is possible to describe the convective flow of air in the

soil as an equation analogous to Darcy's law for water flow, as follows,

$$q = -(k/\lambda) dP/ dx \quad (2.6)$$

where

q = volumetric convective flux of soil gas per unit area in the x -direction,

k = permeability of the air-ksfilled pore space,

λ = viscosity of the soil gas,

P = pressure of the convecting soil gas,

x = direction along which convection occurs.

If the soil gas is assumed an ideal gas and pressure differences are small the nonsteady state flow of a gas through porous media has been presented by Hillel (1980) as,

$$\partial P/ \partial t = \alpha \partial^2 P/ \partial x^2 \quad (2.7)$$

where

P = pressure,

α = composite constant [L^2/ T].

Phenomena that can cause pressure differences in soil gas are barometric pressure changes, temperature gradients, wind gusts over soil surfaces, recharging water, fluctuations of a water table, and extraction of soil water by plant roots (Hillel, 1980). Pressure differences could also be induced by the soil gas sampling procedure.

Advection of Soil Water

Movement of water in the vadose zone can occur by saturated or unsaturated flow. Soil water can move vertically, horizontally, or in some combination depending on the forces acting on it. The water could

also act as either a source or sink for TCE in the vadose zone depending on the origin and history of the water. Possible sources of soil water at the Carranza site include rainfall, recharge from the Santa Cruz River, and liquid wastes. The effect on the soil gas profile depends on the chemical constituents and direction of movement of the recharged waters. Water moving through a system will tend to come into equilibrium with that system. Water with little or no TCE in solution would act as a sink drawing TCE out of the soil gas. The opposite would be true of waters with high concentrations of TCE compared to that in the soil gas.

The presence of perched water tables may also affect the concentration profile of TCE. Perched water tables are areas of saturation with unsaturated conditions existing both above and below. The occurrence of low-permeability clay layers in high-permeability sand formation can lead to perched water tables (Freeze and Cherry, 1979). This occurs because clay is less permeable than sand.

A zone of saturation could affect the TCE concentration by acting as a barrier, retarding, or even completely stopping vertical diffusion because of the lack of air pore space. When a local restrictive layer is encountered by a diffusing gas, a horizontal concentration gradient could be produced.

Distribution of TCE between the Gas, Liquid, and Solid Phases

Gases diffusing through the vadose zone will interact with the liquid and solid phases of the soil. Gases will dissolve into the

liquid phase and adsorb onto the solid phase. The distribution of TCE depends on the interactions of the gas, liquid, and solid phases and includes solubility, adsorption, moisture content, organic content, and clay content. Table 2.2 gives a list of some of the properties of TCE.

Solubility of a gas is the maximum amount that will dissolve in pure water at a specific temperature and pressure. More important for gases is Henry's law, equation 2.8, which states that the mass of a slightly soluble gas that dissolves in a definite mass of a liquid at a

TABLE 2.2

Some properties of TCE

Property	
Molecular Weight	131.4
State at 25 °C, 1 atm.	liquid
Melting Point, °C, 1 atm.	-73.0
Boiling Point, °C, 1 atm.	87.0
Solubility in water (mg/l) at 25 °C, 1 atm.	1100
Critical Pressure (atm.)	48.3
Critical Temperature (°K)	574.0
Vapor Pressure 25 °C, (atm.)	0.0631
Gas/Liquid Distribution Coef. (ug/l of gas)/(ug/l of water)	0.35

given temperature is very nearly proportional to the partial pressure of that gas. This holds for gases which do not react chemically with the solvent. Henry's law is,

$$K_{wvoc} = [VOC] / P_{voc} \quad (2.8)$$

where

[VOC] = aqueous concentration of VOC,

P_{voc} = partial pressure of VOC,

K_{wvoc} = gas/liquid distribution coefficient of the VOC.

The adsorption process is a physical or chemical bonding between the solute and the solid substrate. It is a surface phenomenon and may be significant in clays because of their high specific surface areas, and in soils with high organic matter (Lyman et al., 1982).

In the Carranza study the partitioning of TCE among the three phases will be described by the air/soil distribution coefficient, K_S , defined by Marrin (1984) as the ratio of the halocarbon concentration in the headspace (air) of the reaction vial and the halocarbon concentration in the soil/water fraction of the reaction vial at equilibrium. The air/soil distribution coefficient lumps together the effects of solubility and adsorption. Table 2.3 lists the values for K_S calculated from laboratory experiments by Marrin (1984). The values of K_S as a function of degree of saturation were incorporated into the simulations.

TABLE 2.3

Air/soil distribution coefficient (K_s) for TCE measured over varying degrees of saturation (Marrin, 1984).

Degree of Saturation	K_s
0%	0.0
20%	0.043
40%	0.14
60%	0.96
80%	0.90
100%	0.16

Relative Importance of Parameters

Molecular Diffusion

In simulating the distribution of TCE in the vadose zone at the Carranza site the mass transfer of TCE by molecular diffusion was based on Fick's second law, equation 2.2.

Mass transfer of TCE vapor resulting from thermal gradients was not considered in the simulations because of the small temperature gradients (Table 2.4) measured during the Carranza study.

Counter diffusion effects resulting from evaporation of soil water and surface wind action were not considered in the model. These effects are only important in the first meter or two below land surface (Weeks et al., 1982).

TABLE 2.4

Average temperatures and standard deviations measured at the Carranza site at depths of the gas sampling apparatus during the months of August and September, 1984. Listed temperatures are averages of 23 samples.

Depth (m)	Temperature (°C)	Standard Deviation (°C)
1.5	26.9	0.19
3.0	24.5	0.03
7.5	22.1	0.01
13.5	23.0	0.00
22.5	23.9	0.00

Effective Diffusion Coefficient

The effective diffusion coefficient, D_e , used in the model was calculated as follows from the soil water content data, estimations of porosity, and the general diffusion coefficient.

The water content, W_c , can be described by the following equation:

$$W_c = \text{mass water} / \text{mass solids} \quad (2.9)$$

and

$$\text{mass water} = \text{Vol} (n - n_a) \rho_w \quad (2.10)$$

$$\text{mass solids} = \text{Vol} (1 - n) \rho_s \quad (2.11)$$

where

Vol = total volume,

n = total porosity, ratio of pore volume to total volume of soil,

n_a = air porosity, ratio of volume of gases to total volume of soil,

ρ_w = density of water,

ρ_s = density of solids.

Substituting equations 2.11 and 2.12 into 2.10 and rearranging yields:

$$\text{Vol } (n - n_a) \rho_l = W_C \text{ Vol } (1 - n) \rho_S \quad (2.12)$$

Solving for n_a gives

$$n_a = n - [W_C (1 - n) (\rho_S / \rho_l)] \quad (2.13)$$

In calculating values of n_a , ρ_S was assumed equal to 2.65 g/ cm³ and ρ_W was assumed equal to 1.00 g/ cm³. Porosity values were estimated from values listed in Freeze and Cherry (1979), and from the grain size distribution (Table 2.5), calculated by sieve analysis from soil samples collected during drilling.

The general diffusion coefficient, D_{ab} , was calculated from equation 2.3 to be 0.090 cm²/ sec, using the following values,

$$P_{C \text{ air}} = 37.03 \text{ atm,}$$

$$T_{C \text{ air}} = 131.9 \text{ }^\circ\text{K,}$$

$$M_{\text{air}} = 28.97 \text{ g/ moles,}$$

$$P_C \text{ TCE} = 48.30 \text{ atm,}$$

$$T_C \text{ TCE} = 574.0 \text{ }^\circ\text{K,}$$

$$M \text{ TCE} = 131.4 \text{ g/ moles,}$$

$$P = 0.92 \text{ atm,}$$

$$T = 293.0 \text{ }^\circ\text{K,}$$

To estimate D_e from D_{ab} the following equation proposed by Millington (1959) was used,

$$D_e = (n_a / n)^2 n_a^{4/3} D_{ab} \quad (2.14)$$

Equation 2.15 incorporates a pore size distribution and accounts for the change in D_e at low values of air porosity.

TABLE 2.5

Grain size distribution for different depths at the Carranza site.

Depth (m)	% gravel	% sand	% silt and clay
1.5	7	36	57
3.0	20	33	47
4.5	5	55	40
6.0	4	37	59
7.5	1	31	68
9.0	57	15	28
10.5	3	64	33
12.0	57	36	7
13.5	29	64	7
15.0	48	44	8
16.5	23	58	19
18.0	6	20	74
19.5	4	44	52
21.0	0	43	57
22.5	1	28	71
24.0	3	64	33
25.5	2	82	16
27.0	0	35	65

This equation also assumes that the diffusing gas has a low solubility in water. Values of W_c , n_a , n , and D_e for various depths are listed in Table 2.6.

Apparent Diffusion Coefficient

The effective diffusion coefficient, D_e , can be used for diffusion of nonreactive gases through porous media. Practical cases of nonreactive gases in the presence of soil water are hard to find. When the diffusing gas reacts with either the solid phase or liquid phase of the soil, an apparent diffusion coefficient, D_a , must be used. D_a is related to D_e by the following equation,

$$D_a = D_e * R \quad (2.15)$$

with

$$R = \text{Vol}_{\text{gas}} / \text{Vol}_{\text{eq}} \quad (2.16)$$

and

$$\text{Vol}_{\text{eq}} = \text{Vol}_{\text{gas}} + (\text{Vol}_{\text{liq}} + \text{Vol}_{\text{sol}}) / K_s \quad (2.17)$$

where

R = retardation factor,

Vol_{gas} = volume of gas in a unit volume,

Vol_{liq} = volume of liquid in a unit volume,

Vol_{sol} = volume of solid in a unit volume,

Vol_{eq} = space available in a unit volume of soil for TCE to be in the gas phase, adsorbed on the solid phase, or absorbed into the liquid phase.

The retardation factor, R , is so called because the sorption/desorption of a diffusing gas with the porous media will slow or retard the rate of diffusion. The magnitude of retardation of the diffusing

TABLE 2.6

Values of water content (W_c), porosity (n), air-filled porosity (n_a), degree of saturation (S), air/soil distribution coefficient (K_s), and effective diffusion coefficient (D_e).

Depth (m)	W_c	n	n_a	S	K_s	D_e (m^2/day)
1.5	0.05	0.35	0.26	0.26	0.30	7.12 E-2
3.0	0.02	0.35	0.32	0.10	0.40	1.42 E-1
4.5	0.03	0.30	0.24	0.20	0.04	7.43 E-2
6.0	0.08	0.20	0.03	0.85	0.50	1.63 E-4
7.5	0.12	0.30	0.08	0.73	0.92	1.91 E-3
9.0	0.06	0.30	0.24	0.20	0.04	7.43 E-2
10.5	0.14	0.30	0.04	0.87	0.50	1.89 E-4
12.0	0.03	0.30	0.24	0.20	0.04	7.43 E-2
13.5	0.03	0.30	0.24	0.20	0.04	7.43 E-2
15.0	0.03	0.30	0.24	0.20	0.04	7.43 E-2
16.5	0.11	0.25	0.03	0.88	0.50	1.04 E-4
18.0	0.13	0.30	0.06	0.80	0.90	7.31 E-4
19.5	0.16	0.35	0.07	0.80	0.90	8.98 E-4
21.0	0.17	0.35	0.06	0.83	0.90	5.37 E-4
22.5	0.16	0.35	0.07	0.80	0.90	8.98 E-4
24.0	0.09	0.30	0.13	0.57	0.90	9.62 E-3
25.5	0.06	0.30	0.19	0.37	0.13	3.41 E-2
27.0	0.13	0.30	0.06	0.80	0.90	7.31 E-4

gas depends on the ratio of the mobile gas phase to the immobile liquid and solid phase plus the mobile gas phase. TCE does not partition among the three phases equally but according to the air/soil distribution coefficient. The Vol_{eq} represents space available in a unit volume of soil for TCE to be in the gas phase, adsorbed on the solid phase, or absorbed into the liquid phase.

Advective Gaseous Flow

Advective gaseous flow in the vadose zone could occur because of a fluctuating water table, a moving wetting front from recharged water, barometric pressure fluctuations, or be induced by the soil gas sampling apparatus.

The effect of fluctuations in the elevation of the water table are likely to be unimportant if the water table is deep and fluctuations are minor. Freeze and Cherry (1979) have summarized the mechanisms that lead to fluctuations in groundwater levels. Fluctuations of the water table have not been documented at the Carranza site and were not included in the simulations.

If rainfall is of large areal extent and magnitude it could create pressure changes and advective gaseous flow in the vadose zone by a capping effect caused by a decrease in air porosity. Recharging water would cause a decrease in air porosity and an increase in the soil gas pressure where soil gas is displaced by recharging water. Precipitation and changes in TCE concentrations at the Carranza site during the months of August and September, 1985, showed no discernable correlation. Any

effect rainfall might have on the TCE distribution in the vadose zone was not included in the computer simulations.

The barometric pressure change over a six-hour period at land surface and at various depths (Figure 2.1) was measured at the Carranza site with an inclined barometer, the same one used by Weeks (1978) to determine vertical permeability to air in the vadose zone.

The effect of a diurnal barometric pressure change was simulated by superimposing its effect over a diffusing system. The mass transfer by barometric pressure changes was calculated by using the ideal gas law,

$$P V = n R T \quad (2.18)$$

where

P = pressure,

V = volume,

n = number of moles of gas,

T = absolute temperature,

R = universal gas constant per mole.

If over a length of time, the barometric pressure changes from P_1 to P_2 , then

$$P_1 V_1 / n R T = P_2 V_2 / n R T \quad (2.19)$$

If n and T are assumed constant equation 2.20 reduces to,

$$P_1 V_1 = P_2 V_2 \quad (2.20)$$

If V_1 is taken to be a unit volume of soil gas the volume change, $V_1 - V_2$, produced by the barometric pressure change, $P_1 - P_2$, can be calculated. This volume change can be considered the volume of air moving

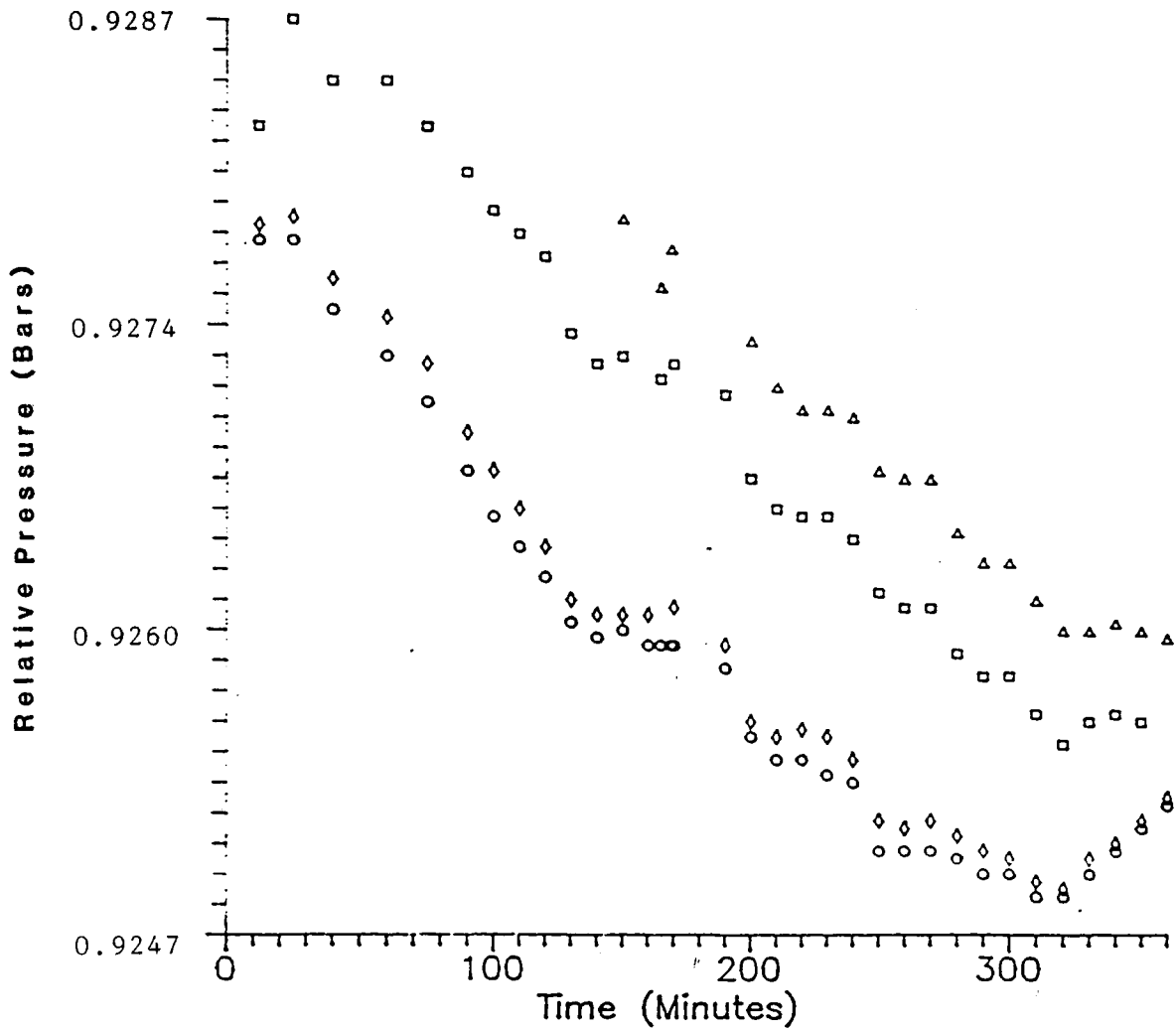


Figure 2.1 Barometric pressure at the Carranza site after noon on 10-13-84 at land surface (circles), at a depth of 7.5 m (diamonds), at a depth of 11.5 m (squares), and at a depth of 22.5 m (triangles).

in to or out of the unit volume of soil due to the barometric pressure change.

In the computer simulation, $P_1 = 0.999$ bars, $P_2 = 0.995$ bars, and $V_1 = 27.4 \text{ m}^3 * 0.14$, where 0.14 is the average air porosity calculated from Table 2.6. V_1 and V_2 were calculated considering a column of soil of area 1 m^2 with a depth of 27.4 m. Inserting these values into equation 2.19 and solving for $V_1 - V_2$ a value of 0.014 m^3 is calculated for the volume of air moving in to or out of the 27.4 m^3 of soil. Barometric pressure fluctuations were incorporated into the simulations in this fashion.

Induced movement of soil gas by collection of samples was held to a minimum by keeping sample volumes to a minimum. The largest amount sampled was equal to three times the volume of the longest sampling line length, approximately 300 ml. Turin (1986) checked for interconnections between sampling stations at the Carranza site by comparing two different sampling techniques including the one described above and another that pumped relatively large volumes of soil gas before sampling. He found that only when pumping large amounts of soil gas at the deepest station did a mixing of soil gas of this station occur with that of a shallower station.

Advection of Water

Advection of water was not considered in the simulation of the Carranza site. No datum was available on advection of water or whether the moisture profile was changing during the study. Water content values, determined from split-spoon samples during drilling, were considered constant in the simulations studies.

Hargis and Montgomery (1982) found, in the vicinity of the Tucson International Airport, perched water tables up to 405 km² in area and from 0.5 to 1.5 meters thick, at depths of 15.2 to 21.3 meters below land surface. The layers supporting the perched water tables consisted of sandy clay and clay. Marrin (1984) found saturated zones at depths below 17.2 meters. He believed this was a possible cause for his anomalous soil gas concentration profile and that air porosity of the porous media was the most important parameter in determining the effective diffusion coefficient. Perched water tables are taken into account in the simulation by using a low air porosity value in calculating the effective diffusion coefficient for depths at which air porosity was small.

CHAPTER 3

DISCRETE-STATE COMPARTMENT MODEL

Introduction

The Discrete-State Compartment (DSC) model is a discretized version of the cells-in-series (CIS) models first developed by chemical engineers (Himmelblau and Bischoff, 1968). The CIS models are solved by obtaining analytical solutions of the governing differential equations and are limited to a few relatively simple cases. The DSC model allows for nonuniform compartment characteristics and is solved by iteration of a recursive mass-balance equation. Dr. E. S. Simpson, of the University of Arizona, first programmed the DSC model on a Wang desk-top calculator in 1971. The original program code was written in Fortran IV by M. E. Campana (1975) and has since been modified in Fortran 77 for the purpose of execution on personal computers.

The DSC model is powerful because of its flexibility and ability to be run on personal computers. The DSC model is flexible because the hydrologic system being modeled is discretized into a network of interconnected compartments. Each compartment can vary in all physical parameters, including porosity, air porosity, water content, and distribution coefficients. The network of compartments can be arranged in 1-, 2-, or 3-dimensional arrays. Volumes of individual compartments can differ from one to another, and the volume of individual compartments can change, if

need be, from one iteration to the next. Inputs to and outputs from the model can be made from any compartment and inputs can vary with time (i.e., from one iteration to the next). The DSC model tracks the movement of a numerical tracer through the network of compartments by iterating a recursive mass-balance equation. A concentration gradient can exist among compartments, but in each individual compartment the numerical tracer is completely mixed, hence the DSC model is also termed a "mixing-cell" model. Radioactive decay, first-order chemical reactions, and age distribution are included in the DSC model. The DSC model is programmed for use on a personal computer which saves time and money because use of a mainframe computer is not needed. The DSC computer code is easy to understand and additional features can be easily added to the model.

Operation of the DSC Model

The common starting point in describing the transport of gases in porous media is to consider the mass flux of a solute into and out of a fixed elemental volume within the hydrologic system. A conservation of mass equation for this elemental volume would be

$$\begin{array}{rclcl} \text{net rate of} & & \text{flux of} & & \text{flux of} & & \text{loss or gain} \\ \text{change of mass} & = & \text{solute out} & - & \text{solute} & \pm & \text{of the solute} \\ \text{of solute} & & \text{of the} & & \text{into the} & & \text{mass due to} \\ \text{within the element} & & \text{element} & & \text{element} & & \text{reactions} \end{array}$$

The transport processes that control the mass flux through the elemental volume in the DSC model are advection and diffusion. The DSC model solves the conservation of mass equation by employing two different subroutines, one subroutine for the advection component and another for

the diffusion component of the mass flux. The advective subroutine is appropriate when the movement of fluid and solutes from one compartment to another occurs as the result of a fluid velocity field. The diffusion subroutine is appropriate when solute movement occurs because of the presence of concentration gradients. The two subroutines can be combined for applications where both processes occur simultaneously.

The basic equation used by the DSC model is a conservation of mass equation written so that inputs, outputs, and sources and sinks within compartments are combined, and is,

$$S(x,n+1) = S(x,n) + BRV(x,n) * BRC(x,n) - BDV(x,n) * BDC(x,n) \pm R(x,n) \quad (3.1)$$

where

$S(x,n)$ = the mass of solute in compartment x at iteration n ,

$BRV(x,n)$ = the boundary recharge volume (input volume of fluid to compartment),

$BRC(x,n)$ = the boundary recharge concentration (input concentration of solute),

$BDV(x,n)$ = the boundary discharge volume (output volume of fluid from compartment),

$BDC(x,n)$ = the boundary discharge concentration (output concentration of solute),

$R(x,n)$ = the sum of solute sources (positive) and/or sinks (negative) within the compartment.

All terms of equation 3.1 are known or assigned except the boundary discharge concentration, BDC . Two different mixing algorithms are available to solve for the BDC in the advection subroutine and the diffusion subroutine and are described in the following sections.

Advection Subroutine

Movement of substances from one compartment to another by advection can be solved by the DSC model using two different algorithms. Each algorithm solves for the BDC of a compartment, which is necessary for the mass balance equation. The first algorithm is termed the simple mixing cell (SMC) and is described by the following equation,

$$\text{BDC}(x,n+1) = \frac{[S(x,n) + \text{BRV}(x,n) * \text{BRC}(x,n)]}{[\text{VOL}(x,n) + \text{BRV}(x,n)]} \quad (3.2)$$

where $\text{Vol}(x,n)$ = the volume of compartment x at iteration n .

The BDC is calculated by assuming that at each iteration the compartment walls expand to accommodate the incoming fluid (Figure 3.1, upper illustration). The incoming fluid is then completely mixed with the fluid of the compartment. The compartment then contracts to its original volume discharging an equal volume of fluid from the compartment to other compartments inside the system, or to the outside environment. The BDC will be equal to the concentration of the substance in the compartment at its expanded condition. The algorithm may be described as a input-mix-output process.

The second algorithm is termed the modified mixing cell (MMC) and is described by the following equation,

$$\text{BDC}(x,n+1) = S(x,n) / \text{VOL}(x,n) \quad (3.3)$$

The MMC algorithm assumes that the incoming fluid first displaces an equal volume of fluid (Figure 3.1, lower illustration), and then mixes with the remaining fluid in the compartment. The BDC will be equal to the substance concentration of the compartment at the given iteration. The algorithm can be described as a input-output mix process.

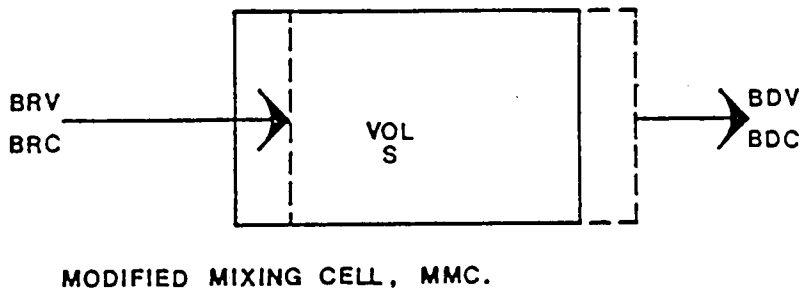
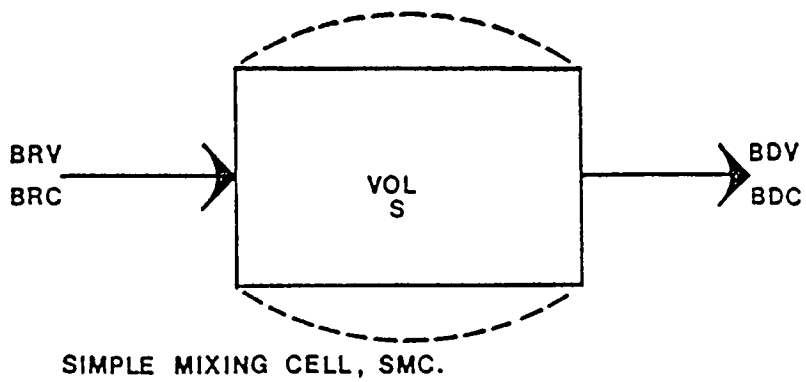


Figure 3.1. Stepwise operation of two advection algorithms by DSC model (Rasmussen, 1982).

Exchange Subroutine

The exchange algorithm allows for modeling mass transfer of solute without net fluid transport. There are two algorithms for exchanges. With the SMC algorithm, a volume of fluid and tracer is first moved from one compartment and mixed with the next (Figure 3.2, upper illustration). After mixing, an equivalent amount of fluid is moved back to the original compartment and mixed. The operation would be an input-mix-output-mix algorithm. The operation can be described analytically by taking the difference between the mass transported from the first compartment to the second compartment and subtracting the mass transported back from the second compartment to the first as indicated below:

$$M_1 = R_i * S(1,n) / VOL(1,n) \quad (3.4)$$

$$M_2 = R_i * (M_1 + S(2,n)) / (R_i + VOL(2,n)) \quad (3.5)$$

$$M = M_1 - M_2 \quad (3.6)$$

$$= R_i * [S(1,n)/VOL(1,n)] - [S(1,n)/VOL(1,n) + S(2,n)] / (R_i + VOL(2,n)) \quad (3.7)$$

where

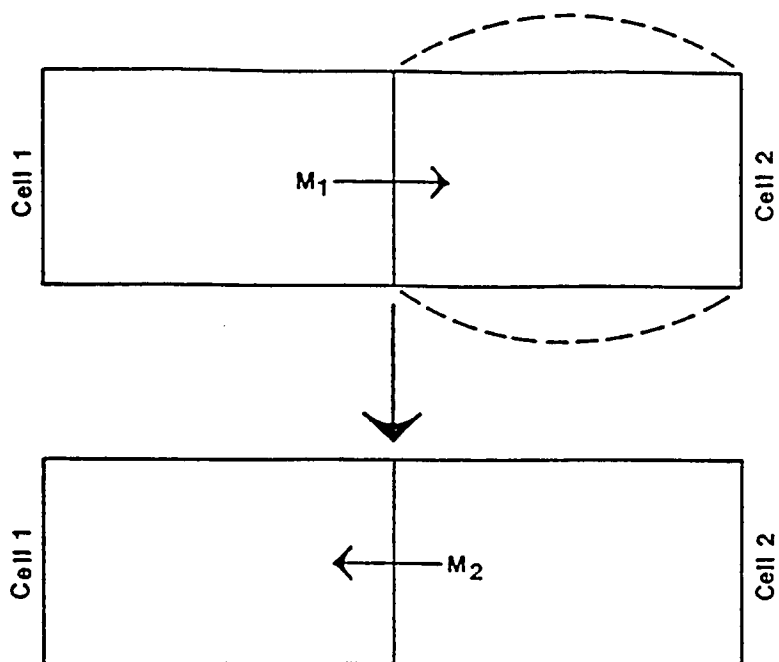
R_i = the exchange volume, which is the volume transported from the first compartment to the second and then back to the first,

M_1 = the mass transported from compartment 1 to compartment 2,

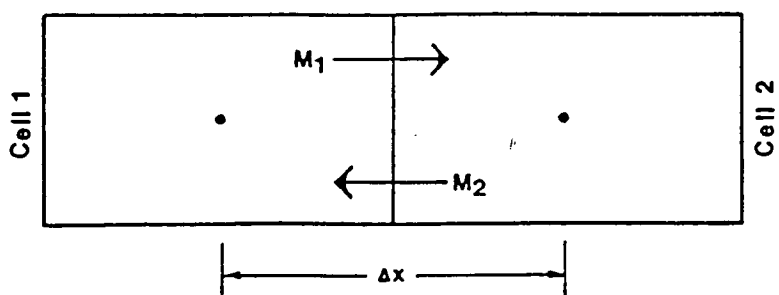
M_2 = the mass transported from compartment 2 to compartment 1,

M = the net mass flux between the two compartments.

The second option is the MMC algorithm. The MMC operation exchanges equal volumes of fluid before mixing (Figure 3.2, lower illustra-



SIMPLE MIXING CELL, SMC.



MODIFIED MIXING CELL, MMC.

Figure 3.2. Stepwise operation of two exchange algorithms by DSC model (Rasmussen, 1982).

tion). The procedure would be an input-output-mix-mix process, calculated by:

$$M_1 = R_i * S(1,n) / VOL(1,n) \quad (3.8)$$

$$M_2 = R_i * S(2,n) / VOL(2,n) \quad (3.9)$$

$$M = R_i * S(1,n) / VOL(1,n) - S(2,n) / VOL(2,n) \quad (3.10)$$

Barometric Subroutine

A separate subroutine to handle mass transport by barometric pressure fluctuations was incorporated into the DSC model. Based on equation 2.20 the volume of air moving into or out of a unit volume of soil at land surface due to barometric pressure fluctuations was calculated. The volume of air moving was assumed to decrease linearly with depth and was zero at the water table. The mass transfer between compartments was calculated by the following equation.

$$\text{mass} = \text{volume} * \text{conc} \quad (3.11)$$

where

mass = mass of substance transported between compartments,

volume = volume of soil gas calculated to be displaced between compartments by the barometric pressure fluctuation,

conc = concentration of substance in volume of soil gas displaced.

Applications of the DSC model

The DSC model has been applied in many different situations. Campana (1975) used carbon-14 age distribution in a portion of the Tucson Basin aquifer to calibrate a 3-D steady-state model. He used the space-time distribution of tritium peaks in the Edwards limestone aquifer of

Texas to calibrate a 2-D transient model. The Edwards limestone is karstic and difficult to model by other methods.

Rasmussen (1982) used the DSC model to simulate solute transport in saturated fractured rock where matrix diffusion occurred. He demonstrated that the DSC model produced results essentially identical to results obtained by an analytical solution of the same system. He generalized the relation between Fick's coefficient of diffusion, D , and the exchange parameter, R_i , of the DSC model.

Samper et al. (1985) applied the DSC model to groundwater dating. They found that the DSC model represents a flexible and yet simple tool to deal with real systems in which various mixing processes are taking place.

Roberts (1986) applied the model to a test of the use of fluorinated hydrocarbons as tracers in unsaturated media. She used complementary compartments to represent the gas, liquid, and solid phases of the porous media and a time dependent sorption rate constant.

Osborn (1987) used the DSC model to project groundwater quality in an area with changing land use and an increasing population. Nitrate was used as an indicator of water quality. A modification was made to the DSC to account for the effect of significant groundwater pumping.

Analytical Solution

The DSC model was tested against an analytical solution of Fick's second law to determine the degree to which the DSC solution matches an analytical solution, in order to guide the interpretation of DSC results for complex systems having no analytical solution.

The analytical solution to Fick's second law used in comparison with the DSC model is given by Crank (1975, eq. 4.22) for a system that has a constant coefficient of diffusion, D , has a uniform initial concentration of C_0 , and has constant boundary conditions C_1 and C_2 and is,

$$C = C_1 + (C_2 - C_1) x/d + 2/\pi \sum_{n=1}^{\infty} [C_2 \cos(n\pi - C_1/n)]$$

$$* \sin(n\pi x/d) \exp(-Dn^2\pi^2t/d^2) + 4C_0/\pi \sum_{m=0}^{\infty} (1/2m+1) \sin(2m+1)\pi x/d$$

$$* \exp[-D(2m+1)^2 \pi^2t/d^2] \quad (3.12)$$

where

C = concentration at x for time t ,

C_0 = initial concentration in system,

C_1 = constant concentration at $x = 0$,

C_2 = constant concentration at $x = d$,

d = length of system,

x = spatial coordinate,

t = time,

D = coefficient of diffusion.

For comparison with the DSC model the following values were used in the analytical solution;

t = 25 years,

d = 27.4 meters,

D = 0.001 cm²/sec,

C_0 = 0.0 ug/l,

C_1 = 16.0 ug/l,

C_2 = 0.0 ug/l.

These values were also used in the DSC model. The DSC model also needed the compartment size (Δx), time step (Δt), and porosity defined. Sensitivity analysis was done on these parameters to determine the optimal values for use in the DSC model. It was found that for a homogenous system, the porosity used did not matter. Porosity matters only in determining the apparent diffusion coefficient by equation 2.12.

Table 3.1 compares the analytical solution vs. the DSC model for three different compartment sizes, 249 cm, 83.1 cm, and 27.7 cm, when $\Delta t = 1$ week. It can be seen that as the compartment size decreases, the difference between the results of the analytical solution and DSC model becomes smaller.

Table 3.2 compares the analytical solution and the DSC model for three different time steps, 12 hours, 1 day, and 1 week, when $\Delta x = 27.7$ cm. As the time step decreases the DSC model results more closely match the results of the analytical solution.

The two different mixing algorithms, the SMC and the MMC, are compared in Table 3.3. The DSC model results, using the MMC algorithm, do not closely match the analytical solution when R_i is close to one. This does not occur with the SMC. As R_i becomes $\ll 1$ the MMC more closely approximates the analytical solution (Table 3.4).

Table 3.5 lists the DSC model results, the analytical solution, the difference between them, and the percentage error for $\Delta x = 27.7$ cm and $\Delta t = 1$ day using the SMC.

Values for Δx and Δt are assigned in the next section.

TABLE 3.1

Comparison of the DSC model and the analytic solution, $\Delta t =$ one week.

Depth (m)	$\Delta x = 249$ cm ($\mu\text{g/l}$)	$\Delta x = 83.1$ cm ($\mu\text{g/l}$)	$\Delta x = 27.7$ cm ($\mu\text{g/l}$)	Anal. Sol. ($\mu\text{g/l}$)
1.24	0.312	0.274	0.255	0.232
3.73	0.677	0.725	0.746	0.737
6.23	1.15	1.28	1.33	1.34
8.72	1.78	2.00	2.08	2.12
11.2	2.63	2.93	3.03	3.12
13.7	3.73	4.13	4.25	4.39
16.2	5.12	5.62	5.75	5.95
18.7	6.81	7.41	7.54	7.79
21.2	8.80	9.48	9.61	9.92
23.7	11.0	11.8	11.9	12.3
26.2	13.5	14.2	14.4	14.7

TABLE 3.2

Comparison of the DSC model and the analytic solution, $\Delta x = 27.7$ cm.

Depth (m)	$\Delta t = 12$ hours ($\mu\text{g/l}$)	$\Delta t = 1$ day ($\mu\text{g/l}$)	$\Delta t = 1$ week ($\mu\text{g/l}$)	Anal. Sol ($\mu\text{g/l}$)
1.24	0.250	0.252	0.255	0.232
3.73	0.736	0.741	0.746	0.737
6.23	1.32	1.33	1.33	1.34
8.72	2.08	2.09	2.08	2.12
11.2	3.06	3.07	3.03	3.12
13.7	4.30	4.31	4.25	4.39
16.2	5.84	5.85	5.75	5.95
18.7	7.67	7.67	7.54	7.79
21.2	9.78	9.77	9.61	9.92
23.7	12.1	12.1	11.9	12.3
26.2	14.6	14.6	14.4	14.7

TABLE 3.3

Comparison of the different mixing algorithms of the DSC model for $\Delta x = 27.7$ cm, $\Delta t = 1$ week, and $Ri = 0.788$.

Depth (m)	SMC (ug/l)	MMC (ug/l)	Anal.Sol. (ug/l)
1.24	0.255	0.756	0.232
3.73	0.746	2.12	0.737
6.23	1.33	3.48	1.34
8.72	2.08	4.85	2.12
11.2	3.03	6.22	3.12
13.7	4.25	7.60	4.39
16.2	5.75	8.99	5.95
18.7	7.54	10.4	7.79
21.2	9.61	11.8	9.92
23.7	11.9	13.2	12.3
26.2	14.4	14.6	14.7

TABLE 3.4

Comparison of the different mixing algorithms of the DSC model for $\Delta x = 249$ cm, $\Delta t = 1$ week, and $Ri = 0.00975$.

Depth (m)	SMC (ug/l)	MMC (ug/l)	Anal.Sol. (ug/l)
1.24	0.312	0.318	0.232
3.73	0.677	0.690	0.737
6.23	1.15	1.17	1.34
8.72	1.78	1.81	2.12
11.2	2.63	2.66	3.12
13.7	3.73	3.76	4.39
16.2	5.12	5.16	5.95
18.7	6.81	6.85	7.79
21.2	8.80	8.83	9.92
23.7	11.0	11.1	12.3
26.2	13.5	13.5	14.7

TABLE 3.5

Comparison of the DSC model using the SMC and the analytic solution, $\Delta x = 27.7$ cm and $\Delta t = 1$ day, with the difference and percentage error.

Depth (m)	DSC model ($\mu\text{g/l}$)	Anal. Sol. ($\mu\text{g/l}$)	Difference ($\mu\text{g/l}$)	% Error
1.24	0.252	0.232	0.020	8.62
3.73	0.741	0.737	0.004	0.54
6.23	1.33	1.34	0.010	0.75
8.72	2.09	2.12	0.030	1.42
11.2	3.07	3.12	0.050	1.60
13.7	4.31	4.39	0.080	1.82
16.2	5.85	5.95	0.100	1.68
18.7	7.67	7.79	0.120	1.54
21.2	9.77	9.92	0.150	1.51
23.7	12.1	12.3	0.200	1.63
26.2	14.6	14.7	0.100	0.68

Model Parameter Formulation

The DSC model parameters needed for simulation studies are the compartment system, time step, the initial compartment state, system boundary recharge concentration, exchange factor, and equivalent volume. To the extent possible, assigned values will be based on known field data.

The Compartmental System

Three different compartment systems were designed for computer simulation. A 2-dimensional system of 18 by 5 compartments was used to simulate both horizontal and vertical soil heterogeneities. Two 1-dimensional systems of 100 and 18 compartments were used to simulate only vertical heterogeneities.

The Time Step

From historical records it was postulated that TCE had been moving through the vadose zone for 25 years at the Carranza site. A discretized time step of one week was chosen because it gave results consistent with the analytical solution and required only a modest amount of computer time. When diurnal barometric pressure fluctuations were modeled, a time step of 12 hours was used because it represented close to one half of a diurnal barometric pressure cycle.

Initial Compartment State

An initial compartment state or initial concentration of TCE in the compartment of 0.0 ug/l was used for all scenarios. This assumes

that 25 years ago there was no TCE in the vadose zone at the Carranza Site.

System Boundary Recharge Concentration

Table 3.6 lists values of TCE in samples of groundwater obtained from three sources in close proximity to the Carranza site: (1) The Carranza domestic well used by the residence until closure, (2) the Thomson augered hole, and (3) samples obtained by bailing from the augered hole of this report prior to emplacement of the nest of piezometers

In all simulations a constant value of 100 ug of TCE/ l in groundwater was assumed as reasonable for the purpose of testing various hypotheses. The concentration of TCE in the vadose zone directly above the water table was calculated by multiplying the air/soil partitioning coefficient from Table 2.3 for 100% saturation and the concentration in the groundwater. The SBRC was calculated to be 16.0 ug of TCE/ l of soil gas.

TABLE 3.6

Concentrations of TCE measured in groundwater in proximity to the Carranza site.

location of well	TCE concentration (ug/l)	Date Sampled
Carranza site, bailed	92.0	12/05/83
	78.0	12/06/83
Carranza domestic well	389.0	08/24/84
	319.0	11/28/84
Thomson (1985), bailed	153.0	11/17/84

Exchange Factor

The exchange factor (R_i) is the parameter that gives the percentage of the volume of a compartment that is exchanged or advected between compartments. Its value depends on the transport mechanism being used.

For diffusion, the relationship between R_i and D_e is (Rasmussen, 1982),

$$R_i = D_e * \Delta t / \Delta x^2 \quad (3.13)$$

Where sorption is modeled, an apparent diffusion coefficient, D_a , is used and equation 3.13 becomes,

$$R_i = D_a * \Delta t / \Delta x^2 \quad (3.14)$$

For the mass flux caused by barometric pressure fluctuations,

$$R_i = 1.4 * (1 - d / 27.4) \quad (3.15)$$

where d = the depth below land surface. This equation was developed from equation 2.20. The coefficient, 1.4, is the volume of air per unit area calculated to move into or out of the vadose zone at the land surface from a diurnal barometric pressure change measured at the Carranza site. The relationship implies that the volume of air moving in the vadose zone decreases linearly with depth.

Equivalent Volume of the Compartment

TCE moving through the vadose zone will partition between the gas phase and the liquid/solid phase of the soil according to the distribution coefficient, K_s . The DSC model could simulate the movement of TCE by dividing each compartment into two subcompartments representing the gas phase and the liquid/solid phase. This is not necessary if the volume of the liquid/solid phase is prorated to indicate the partitioning

ratio. When the volume of liquid and solid in a compartment is divided by K_S (see Table 2.6 for values of K_S) the resultant volume, Vol_{res} , is equal to a volume of gas that would contain the same mass of TCE absorbed into the soil water or adsorbed onto the soil. The equation describing this is,

$$Vol_{res} = (Vol_{liq} + Vol_{sol}) / K_S \quad (3.16)$$

where

Vol_{res} = volume of gas that would contain the same mass of TCE absorbed into the soil water or adsorbed onto the soil,

Vol_{liq} = volume of liquid phase of compartment,

Vol_{sol} = volume of solid phase of compartment.

The equivalent volume of the compartment can be calculated by the following equation,

$$Vol_{eq} = Vol_{gas} + (Vol_{liq} + Vol_{sol}) / K_S \quad (3.17)$$

or

$$Vol_{eq} = Vol_{gas} + (Mass_{(l + s)} / Mass_g) * Vol_{gas} \quad (3.18)$$

where

Vol_{eq} = equivalent volume of the compartment,

Vol_{gas} = volume of gas phase of compartment,

$Mass_{(l + s)}$ = mass per unit volume of TCE in liquid and solid phases of the compartment,

$Mass_g$ = mass per unit volume of TCE in the gas phase.

Values of Vol_{eq} , Vol_{gas} , D_a , and R_i used in the computer simulations are listed in Table 3.7.

TABLE 3.7

Values of volume gas, (Vol_{gas}), volume equivalent, (Vol_{eq}), apparent diffusion coefficient, (D_a), and exchange factor (Ri) used in the computer simulations for the different depths.

Depth (m)	Vol_{gas}	Vol_{eq}	D_a (m^2/day)	Ri
1.5	4.4	18.6	1.68 E-2	2.12 E-2
3.0	5.4	34.1	2.25 E-2	7.00 E-2
4.5	4.1	324	9.40 E-4	2.93 E-3
6.0	0.5	33.2	2.45 E-6	7.65 E-6
7.5	1.3	16.9	1.47 E-4	4.57 E-4
9.0	3.2	108	2.20 E-3	3.14 E-3
10.5	0.7	33.1	4.00 E-6	1.24 E-5
12.0	4.1	324	9.40 E-4	2.93 E-3
13.5	4.1	324	9.40 E-4	2.93 E-3
15.0	4.1	324	9.40 E-4	2.93 E-3
16.5	0.5	33.2	1.57 E-6	4.90 E-6
18.0	1.0	18.6	3.93 E-5	1.22 E-4
19.5	1.2	18.6	5.79 E-5	1.80 E-4
21.0	1.0	18.6	2.89 E-5	8.99 E-5
22.5	5.9	18.1	2.93 E-4	9.11 E-4
24.0	2.2	18.5	1.14 E-3	3.56 E-3
25.5	3.2	108	1.01 E-3	3.14 E-3
27.0	1.0	18.6	3.93 E-5	1.22 E-4

CHAPTER 4

SIMULATION STUDIES

Introduction

The simulation studies described in this chapter tested various hypotheses concerning the transport mechanisms of TCE vapor in the vadose zone. The studies were divided into seven different scenarios. The source of the TCE vapor in scenarios 1, 2, 3, and 4 was dissolution from contaminated groundwater, and the transport mechanism was molecular diffusion upward from the water table to the atmosphere. The first four scenarios were different from each other by the heterogeneities simulated by the compartmental system. Scenario 5 simulated a multi-source system for TCE. Sources of TCE were dissolution from groundwater and horizontal diffusion from sources above the water table. Scenario 6 had dissolution from contaminated groundwater as the source of TCE and included advection of soil gas by barometric pressure fluctuations. Scenario 7 added advection of soil gas by barometric pressure fluctuations to the compartmental system used in scenario 2.

Undoubtedly, other hypotheses and scenarios could have been proposed and tested. This report provides a sampling of what might be done based on the limited amount of available field data.

Table 4.1 lists the mean concentrations and standard deviations of soil gas sampled at the Carranza site. Values listed are for

TABLE 4.1

TCE mean concentrations and standard deviations of soil gas samples at the Carranza site at depths of the gas sampling apparatus. The values are based on 23 samples taken from each depth during August and September, 1984.

Depth (m)	Mean Concentration (ug/l)	Standard Deviation (ug/l)
1.5	0.013	0.003
3.0	0.019	0.008
7.5	0.005	0.003
13.5	0.008	0.002
22.5	0.575	0.120

the depths at which the sampling apparatus were located. The values are based on 23 samples taken from each depth during August and September, 1984.

Scenario 1a and 1b

Scenario 1a was based on the following assumptions: (1) The vadose zone was homogenous, (2) the mechanism of TCE transport was molecular diffusion, (3) diffusion was only in the vertical direction, (4) the base of the zone (interface with water table) received a constant source (input) or system boundary recharge concentration (SBRC), (5) the top of the zone (interface with the atmosphere) was an infinite sink, and (6) TCE did not sorb with the liquid or solid phases of the vadose zone. Figure 4.1 illustrates the compartmental system used in scenario 1a.

An effective diffusion coefficient, D_e , of $3.63 \text{ E-}3 \text{ m}^2/\text{day}$ was used in scenario 1a. This D_e was chosen because it caused the concentration, after 25 years, at row one to equal the measured concentration at the same depth. These values were equated to illustrate the magnitude

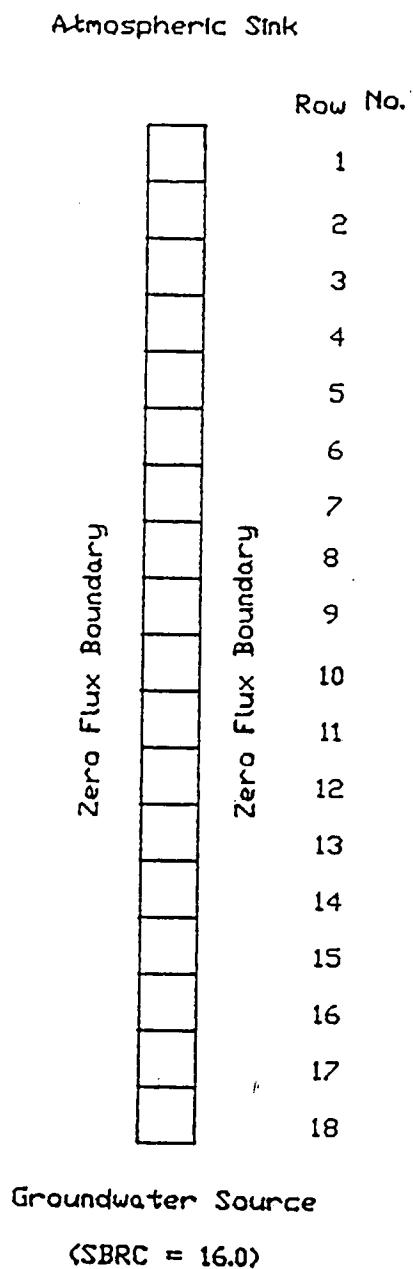


Figure 4.1. Homogenous compartmental system used in scenario 1a. Effective diffusion coefficient = $3.63 \text{ E-}3 \text{ m}^2/\text{ day}$.

of D_e needed to simulate the concentration at the shallowest sampling location. For nonhomogenous systems some average diffusion coefficient would have to be of the same order of magnitude as D_e of scenario 1a to accurately simulate the measured concentration at the shallowest sampling location.

D_e of scenario 1a was orders of magnitude larger than 13 of the 18 apparent diffusion coefficients, D_a , calculated for the Carranza site and listed in Table 4.2. D_e was of the same order of magnitude as the effective diffusion coefficients calculated for the Carranza site and listed in Table 2.6.

Table 4.2 and Figure 4.2 compare TCE concentrations after 25 years with the measured concentrations. The D_e of scenario 1a caused concentrations at the three deepest sampling locations to be orders of magnitude larger than the measured concentrations. Also, the simulated concentration profile, as expected, is monotonically decreasing from the water table to land surface.

TABLE 4.2

TCE concentration (ug/l) profile of scenario 1a after 25 years and the measured concentration profile.

Depth (m)	Row No.	Concentration (ug/l) after 25 years	Measured (ug/l)
1.5	1	1.3 E-2	1.3 E-2
3.0	2	2.9 E-2	1.9 E-2
7.5	5	1.7 E-1	5.0 E-3
13.5	9	1.1	8.0 E-3
22.5	15	7.3	5.7 E-1

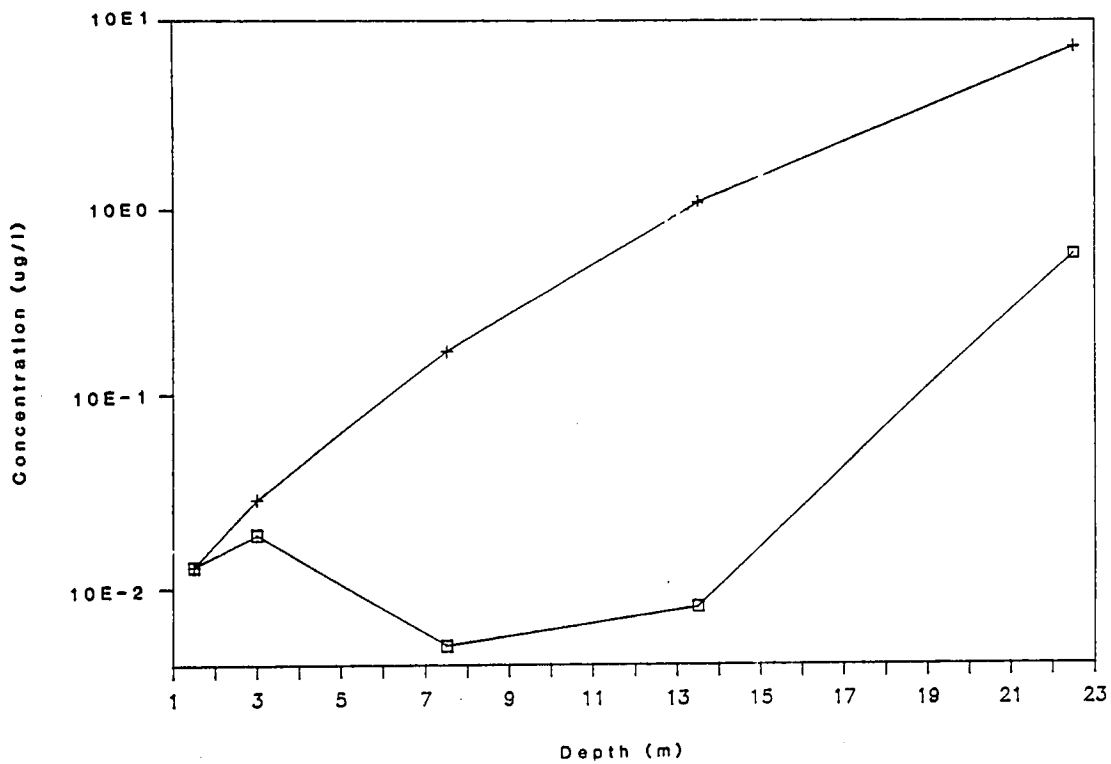


Figure 4.2 TCE concentration (ug/l) profile of scenario 1a after 25 years, plus sign, and the measured concentration profile, squares.

Scenario 1b was based on the same assumptions as scenario 1a except that the base of the zone (interface with water table) received a variable source (input) or system boundary recharge concentration (SBRC). A variable source of TCE at the Carranza site is a more realistic assumption than a constant source but no information on the historic TCE groundwater concentration was available. An arbitrary SBRC, from the groundwater, of 16.0 ug/l from 0 to 5 years, 1600 ug/l from 5 to 10 years, and 16.0 ug/l from 10 to 25 years was chosen. The TCE concentration after 5, 10, 15, 20, and 25 years are listed in Table 4.3.

The concentration profiles after 15, 20, and 25 years indicate that a variable SBRC of TCE from the groundwater can create a non-monotonic concentration profile. The nonmonotonic shape of the concentration profile in scenario 1b was dissimilar to the nonmonotonic shape of the measured concentration profile. The assumptions used in scenario 1b produce a transient concentration profile opposite in the general shape to the measured concentration profile. The highest concentration of TCE in scenario 1b after 15, 20, and 25 years occurred at row number 14 or 15 with lower concentrations occurring at the water table and at land surface. The measured concentration profile had the lowest concentration of TCE at row number five with higher concentrations occurring nearer the water table and land surface.

TABLE 4.3

TCE concentration (ug/l) profile of scenario 1 at different time intervals and the measured concentration profile.

Depth (m)	Row No.	Concentration (ug/l) after				
		5 years	10 years	15 years	20 years	25 years
3.0	2	3.6 E-8	5.8 E-4	6.8 E-3	1.5 E-1	7.9 E-1
7.5	5	5.9 E-6	2.2 E-3	1.8 E-1	1.7	5.4
13.5	9	2.3 E-3	3.0 E-1	7.2	2.3 E+1	3.6 E+1
22.5	15	1.7	1.7 E+2	2.3 E+2	1.6 E+2	1.2 E+2
27.0	18	11.0	1.1 E+4	1.6 E+2	7.9 E+1	5.4 E+1

Scenario 2

Scenario 2 was based on the following assumptions: (1) The vadose zone was homogenous in the horizontal direction but nonhomogenous in the vertical direction, (2) the mechanism of TCE transport was molecular diffusion, (3) diffusion was only in the vertical direction, (4) the base of the zone (interface with water table) received a constant source (input), (5) the top of the zone (interface with the atmosphere) was an infinite sink, and (6) TCE sorbed or desorbed instantaneously. The non-homogenous properties of scenario 2 were based on grain size distribution and water content values of soil samples obtained during drilling (Tables 2.5 and 2.6).

Figure 4.3 illustrates the compartmental system used in scenario 2. The system was a 1-dimensional array of 18 rows. Each row was represented by a single compartment 1.5 m in vertical height and width. Characteristics of each row are listed in Table 2.6. A zero-flux

Atmospheric Sink

Row No.	D_a (m^2/day)
1	1.68 E-2
2	2.25 E-2
3	9.40 E-4
4	2.45 E-6
5	1.47 E-4
6	2.20 E-3
7	4.00 E-6
8	9.40 E-4
9	9.40 E-4
10	9.40 E-4
11	1.57 E-6
12	3.39 E-5
13	5.79 E-5
14	2.89 E-5
15	2.93 E-4
16	1.14 E-3
17	1.01 E-3
18	3.93 E-5

Groundwater Source

(SBRC = 16.0)

Figure 4.3. 1-dimensional system used in scenario 2 with the apparent diffusion coefficient, D_a , shown for individual rows.

boundary was assumed along both sides of the compartmental system.

Table 4.4 compares the concentration profile of scenario 2 for three time intervals with the measured concentration profile. The concentrations listed in Table 4.4 after 25 years are many orders of magnitude lower than those values measured at the Carranza site except at a depth of 22.5 m. The results of scenario 2 indicate that vertical diffusion through horizontally continuous layers with the assigned properties could not produce the concentration profile measured at the Carranza site.

TABLE 4.4

TCE concentration (ug/l) profile of scenario 2 at different time intervals and the measured concentration profile.

Depth (m)	Row No.	Concentration (ug/l) after			Measured (ug/l)
		5 years	15 years	25 years	
1.5	1	1.1 E-31	9.6 E-25	2.0 E-22	1.3 E-2
3.0	2	1.9 E-31	1.3 E-24	1.0 E-21	1.9 E-2
7.5	5	1.1 E-23	4.3 E-18	9.6 E-16	5.0 E-3
13.5	9	1.5 E-17	2.2 E-13	1.2 E-11	8.0 E-3
22.5	15	3.0 E-3	5.0 E-2	1.3 E-1	5.7 E-1

The very low concentrations found in scenario 2 are due to the fact that the rows were modeled as infinitely continuous. No alternate pathway or transport mechanism was available for diffusing TCE to move around rows of small D_a . Once a restrictive row (small D_a) was encountered the mass transfer of TCE was drastically reduced.

The concentration at a depth of 22.5 m was of the same order of magnitude as the measured concentration of the same depth, after 25

years. This sampling station is only 4.5 m above the water table and therefore will equilibrate faster with the TCE concentration in the groundwater than the shallower sampling stations.

With the assumptions on which scenario 2 are based the Carranza site TCE concentration profile could not be generated. With only one constant source and a horizontally homogeneous system monotonically decreasing concentrations from the water table to land surface will always occur.

Scenario 3

Scenario 3 was based on the same six assumptions as scenario 2, except that a high permeable column (HPC) was assumed to exist as shown on Figure 4.4. Hence, molecular diffusion in scenario 3 is 2-dimensional and a 2-dimensional cell system of 5 columns and 18 rows was used. The HPC was assumed to be in column one and the gas sampling apparatus was assumed to be in column five. The properties of the HPC were arbitrarily assigned and are $W_c = 0.03$, $n = 0.35$, $n_a = 0.30$, $S = 0.14$, $K_S = 0.50$, $D_e = 1.15E-1$, $Vol_g = 5.0$, $Vol_{eq} = 28.7$, $D_a = 2.00 E-2$, and $Ri = 5.77 E-1$.

HPCs seldom occur naturally in alluvial deposits but it was added to scenario 2 to illustrate another possible transport pathway for TCE. The alternate pathway made it possible for diffusing gas to move around restrictive rows, rows with small D_a . The HPC fully penetrated the vadose zone. A more complex pathway probably existed, but would not have been more informative than the HPC because no information on the

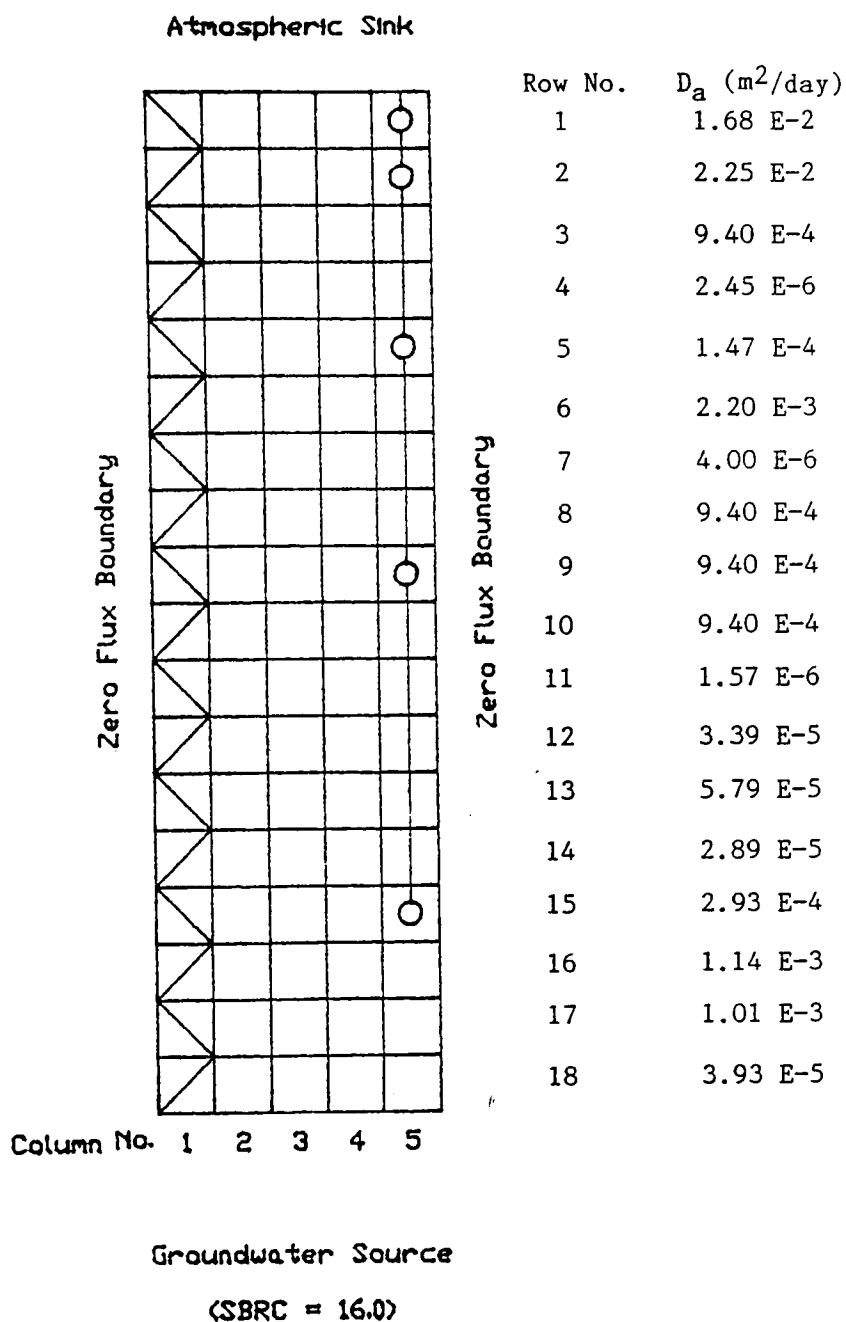


Figure 4.4. Two-dimensional system used in scenario 3, with the apparent diffusion coefficients, D_a , shown for columns 2, 3, 4, and 5 of individual rows. Column 1 represents a high permeable column with $D_a = 2.00 E-2 m^2/day$. Circles represent sampling locations.

horizontal variability of the vadose zone was available. The concentration profiles of scenario 3 at three time intervals are compared with the measured values in Table 4.5. Several interesting results appeared. The concentration profile for $t = 5$ years and $t = 15$ years did not monotonically decrease in concentration from the water table to land surface. This is the same phenomenon that is found with the measured concentration profile. The concentrations at all depths, for $t = 25$ years, are of the same magnitude as the measured concentrations. At 25 years, though, the concentration profile is now monotonically decreasing. The addition of an alternate pathway for the diffusing gas in scenario 3 has caused a 9- to 19-order increase in magnitude of the TCE concentration from scenario 2. The diffusing TCE no longer must solely move through restrictive layers but can, in large part, bypass them. The bypass mechanism also produces the nonmonotonically decreasing profile found at $t = 5$ years and $t = 15$ years by allowing the TCE vapor to move around the 7.5 m and 13.5 m sampling stations.

TABLE 4.5

TCE concentration ($\mu\text{g/l}$) profile of scenario 3 at different time intervals and the measured concentration profile.

Depth (m)	Row No.	Concentration ($\mu\text{g/l}$) after			Measured ($\mu\text{g/l}$)
		5 years	15 years	25 years	
1.5	1	7.6 E-3	1.9 E-3	4.7 E-3	1.3 E-2
3.0	2	1.1 E-4	2.5 E-3	6.2 E-3	1.9 E-2
7.5	5	2.6 E-6	1.5 E-3	1.0 E-2	5.0 E-3
13.5	9	3.8 E-5	6.5 E-3	3.3 E-2	8.0 E-3
22.5	15	4.5 E-2	2.7 E-1	5.7 E-1	5.7 E-1

Scenario 4

In scenario 4 horizontal heterogeneity was added to the system of scenario 3 by changing the R_i value of the center three compartments of selected rows. Figure 4.5 illustrates the location of the HPC, rows with horizontal heterogeneities, and sampling station locations. Changes in the R_i values of the center three compartments of selected rows represented changes in the physical parameters of the vadose zone, water content, porosity, or distribution coefficient. Lacking field data, R_i values were changed arbitrarily.

Table 4.6 lists the rows which had the R_i value of the center three compartments changed. The magnitude of change between scenarios 3 and 4 was small in all cases. A change in water content, porosity, or the distribution coefficient could have accounted for the changes in R_i values. For example at station 7.5 m a decrease in air porosity from 0.08 to 0.06 would give a R_i value of $1.24 \text{ E-}4$. At station 4.5 m a increase of K_s from 0.04 to 0.13 would produce a R_i value of $9.20 \text{ E-}3$. The small changes in R_i values which represent similar small changes in the physical parameters of the row could all be expected to occur in the vadose zone.

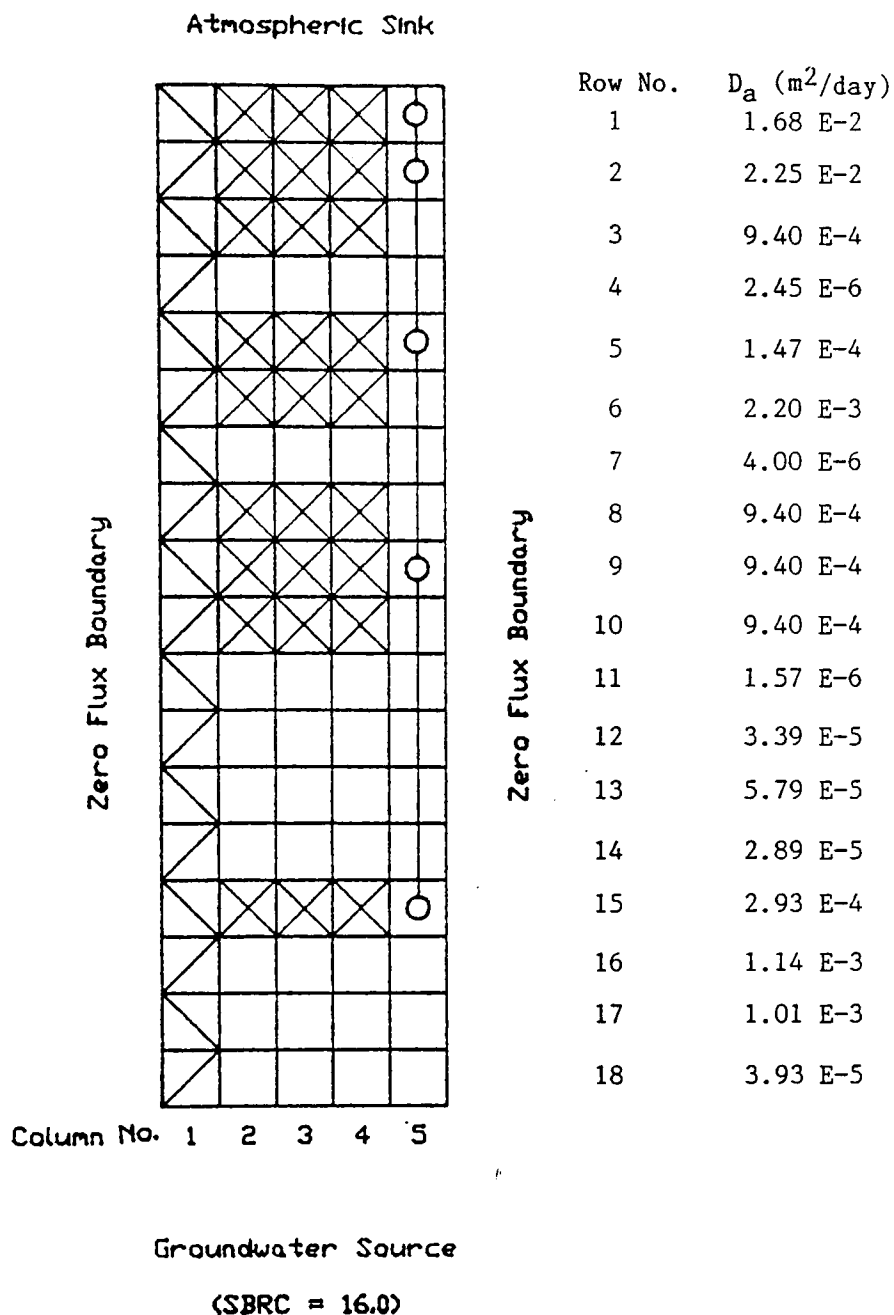


Figure 4.5. Two-dimensional system used in scenario 4, with the apparent diffusion coefficients, D_a , shown for columns 2, 3, 4, and 5 of individual rows. Column 1 represents a high permeable column with $D_a = 2.00 E2$. Circles represent sampling locations. Compartments with x's in columns 2, 3, and 4 had R_i values changed to represent horizontal heterogeneities as listed in Table 4.6.

TABLE 4.6

Rows in which the center three compartments Ri value was changed from scenario 3 to scenario 4 to represent horizontal heterogeneity in the vadose zone.

Depth (m)	Row No.	Ri value scenario 3	Ri value scenario 4
1.5	1	2.12 E-2	2.30 E-2
3.0	2	7.00 E-2	2.39 E-1
4.5	3	2.93 E-3	8.79 E-3
7.5	5	4.57 E-4	1.90 E-4
9.0	6	3.14 E-3	1.90 E-3
12.0	8	2.96 E-3	1.33 E-3
13.5	9	2.96 E-3	1.33 E-3
15.0	10	2.96 E-3	1.33 E-3
22.5	15	9.11 E-4	3.14 E-3

Table 4.7 lists the TCE concentration profile for scenario 4 after 5, 15, and 25 years. The TCE concentration for each of these time spans is nonmonotonically decreasing as the depth decreases. This is similar to the measured concentration profile. As time length increases the difference between concentrations of the four shallowest stations decreases. The profile after 25 years is not yet at steady state. With dissolution from groundwater as the only source of TCE a monotonically decreasing concentration profile must occur before steady state is reached. In scenario 4 it would take 44.2 years before a monotonic concentration profile occurred.

TABLE 4.7

TCE concentration (ug/l) profile of scenario 4 at different time intervals and the measured concentration profile.

Depth (m)	Row No.	Concentration (ug/l) after			Measured (ug/l)
		5 years	15 years	25 years	
1.5	1	2.4 E-4	5.6 E-3	1.2 E-2	1.3 E-2
3.0	2	3.6 E-4	7.5 E-3	1.6 E-2	1.9 E-2
7.5	5	6.0 E-7	5.7 E-4	5.0 E-3	5.0 E-3
13.5	9	2.8 E-6	1.0 E-3	7.7 E-3	8.0 E-3
22.5	15	4.5 E-2	2.8 E-1	5.8 E-1	5.8 E-1

Scenario 5

Scenario 5 was based on the same assumptions as scenario 2, except that additional sources of TCE were included at intermediate depths above the water table as shown in Figure 4.6. Molecular diffusion in this scenario is 2-dimensional and a 2-dimensional cell system of 5 columns and 18 rows was used. The additional sources simulated the effect of possible horizontal TCE gradients in the vadose zone. Lacking field data, the gradients chosen were arbitrary. The source terms used were small compared to those values found in the groundwater and also to concentrations found in soil gas by Marrin (1984) that are listed in Table 1.1.

During each iteration of scenario 5 the non-zero SBRC was mixed with a compartment in column one of each selected row. In column five of the same row a SBRC of 0.0 was mixed. This produced a horizontal gradient through the row and simulated lateral diffusion. At the same time, the model simulated the effect of vertical diffusion upward from

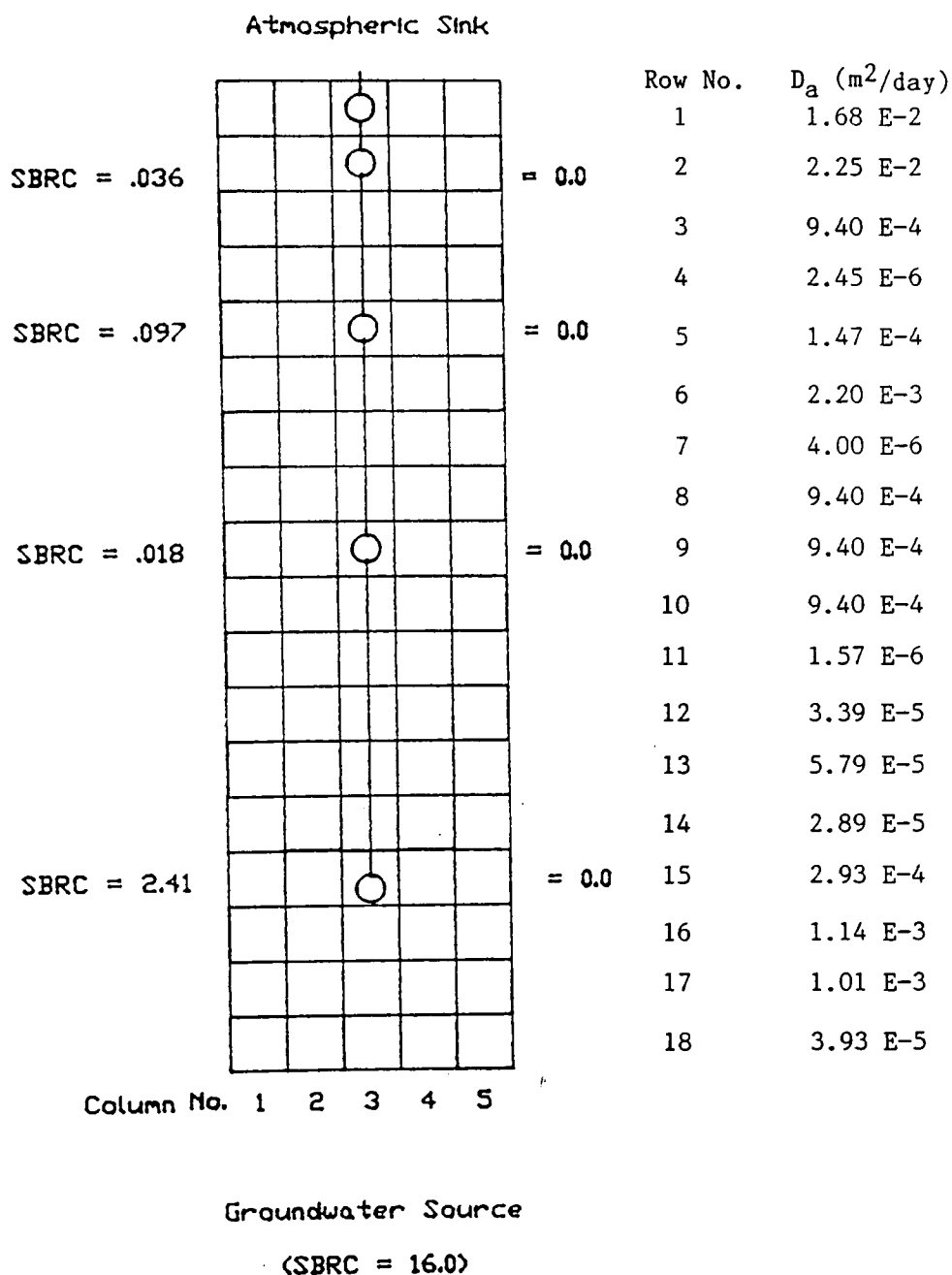


Figure 4.6. Two-dimensional system used in scenario 5 with the apparent diffusion coefficients, D_a , shown for individual rows and location of system boundary recharge concentrations (SBRC) used to simulate lateral diffusion.

the water table. The concentration of the center compartment of a row was considered the sampling station location.

Table 4.8 lists the TCE concentration profile for scenario 5 after 5, 15, and 25 years. With additional sources at intermediate depths, the concentrations after 5 years, 15 years, and 25 years are of the same magnitude as the measured concentration profile and are nonmonotonic.

TABLE 4.8

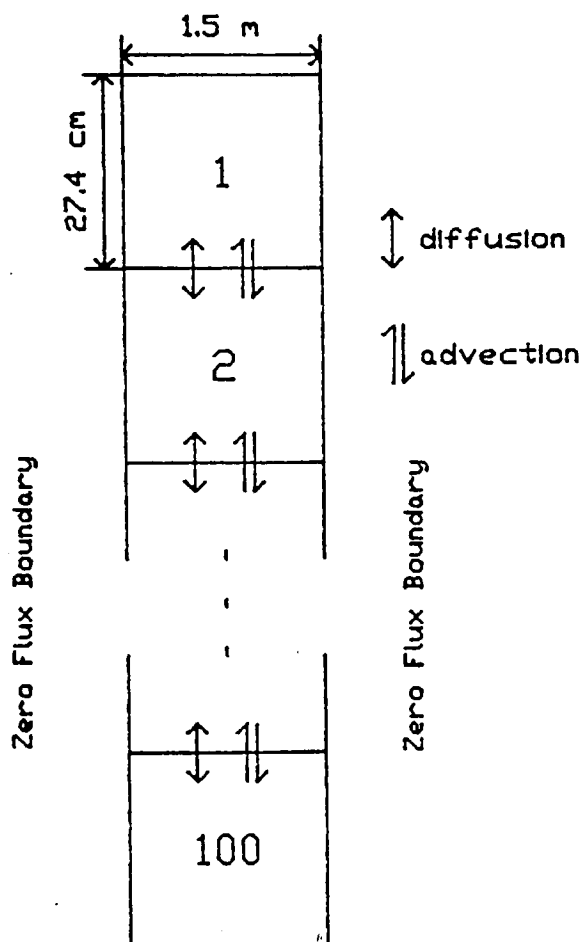
TCE concentration (ug/l) profile of scenario 5 at different time intervals and the measured concentration profile.

Depth (m)	Row No.	Concentration (ug/l) after			Measured (ug/l)
		5 years	15 years	25 years	
1.5	1	1.1 E-2	1.2 E-2	1.2 E-2	1.3 E-2
3.0	2	1.7 E-2	1.9 E-2	1.9 E-2	1.9 E-2
7.5	5	2.8 E-3	4.2 E-3	5.1 E-3	5.0 E-3
13.5	9	5.0 E-3	7.1 E-3	8.2 E-3	8.0 E-3
22.5	15	3.0 E-1	4.6 E-1	5.8 E-1	5.8 E-1

Scenario 6

Scenario 6 was based on the same assumptions as scenario 2, except that a vertical advection of soil gas, caused by diurnal barometric fluctuations, was included with diffusion from the water table. The compartmental system of scenario 6 (Figure 4.7) was 1-dimensional and composed of 100 rows, with the distance between centers of compartments 27.4 cm. A time step of 12 hours was chosen because it is approximately 1/2 of a diurnal barometric pressure cycle.

Atmospheric Sink



Groundwater Source

(SBRC = 16.0)

Figure 4.7. One-dimensional system of scenario 6 used to simulate gaseous diffusion and barometric pressure fluctuations causing gaseous advection.

Scenario 6 was divided into two parts, based on the transport mechanisms used: (6a) gaseous diffusion, and (6b) gaseous diffusion and gaseous advection. Hence scenarios 2 and 6a, are identical except for the number of rows used in the scenario.

Table 4.9 shows the results of scenario 6a, gaseous diffusion at different time intervals. After 25 years the simulated concentrations at four of the Carranza sampling stations (1.5 m, 3.0 m, 7.5 m, and 13.5 m) are 7 to 23 orders of magnitude lower than concentrations measured at the Carranza site. Only the 22.5 m sampling station was of the same order of magnitude as the concentration measured at the Carranza site. Concentrations differed between scenarios 2 and 6a, because with an increase in the number of rows in scenario 6a, there is a decrease in the numerical dispersion of the model.

Table 4.10 shows the results of part 6b, when advection of the soil gas caused by barometric pressure fluctuations was added to the diffusional system of part a.

TABLE 4.9

Concentrations for scenario 6a, gaseous diffusion in a heterogenous system at different time intervals and the measured concentration profile.

Depth (m)	Row No.	Concentration (ug/l) after			Measured (ug/l)
		5 years	15 years	25 years	
1.5	1	0.0	4.4 E-32	4.4 E-25	1.3 E-2
3.0	2	0.0	8.5 E-32	6.7 E-25	1.9 E-2
7.5	5	2.0 E-35	1.1 E-20	9.5 E-15	5.0 E-3
13.5	9	1.6 E-22	4.2 E-13	8.3 E-10	8.0 E-3
22.5	15	2.1 E-2	2.7 E-1	5.4 E-1	5.8 E-1

TABLE 4.10

Concentrations for scenario 6b, gaseous diffusion and gaseous advective transport in a heterogenous system at different time intervals and the measured concentration profile.

Depth (m)	Row No.	Concentration (ug/l) after			Measured (ug/l)
		5 years	15 years	25 years	
1.5	1	1.8 E-19	1.6 E-19	3.2 E-7	1.3 E-2
3.0	2	4.1 E-14	2.9 E-9	4.8 E-7	1.9 E-2
7.5	5	1.3 E-9	1.2 E-6	8.1 E-5	5.0 E-3
13.5	9	2.2 E-2	1.2 E-4	2.0 E-3	8.0 E-3
22.5	15	2.2 E-2	4.7 E-1	9.5 E-1	5.8 E-1

Addition of advection in 6b caused an increase in concentrations compared with 6a at all of the sampling stations. At 22.5 m and 13.5 m the concentrations are of the same order of magnitude as the measured concentrations. At 1.5 m, 3.0 m, and 7.5 m the concentrations are several orders of magnitude below the measured concentrations.

Figure 4.8 compares graphically the calculated concentration profile of scenario 6b after 25 years and the measured concentration profile.

Scenario 7

Scenario 7 was based on the same assumptions as scenario 3, except that advection caused by barometric pressure fluctuations was included. In scenario 3 a high permeable column had been added to the layered compartmental system of scenario 1. Table 4.11 and Figure 4.9 compare the concentrations of scenario 7 with and without barometric pressure fluctuations after 25 years and the measured concentration profile.

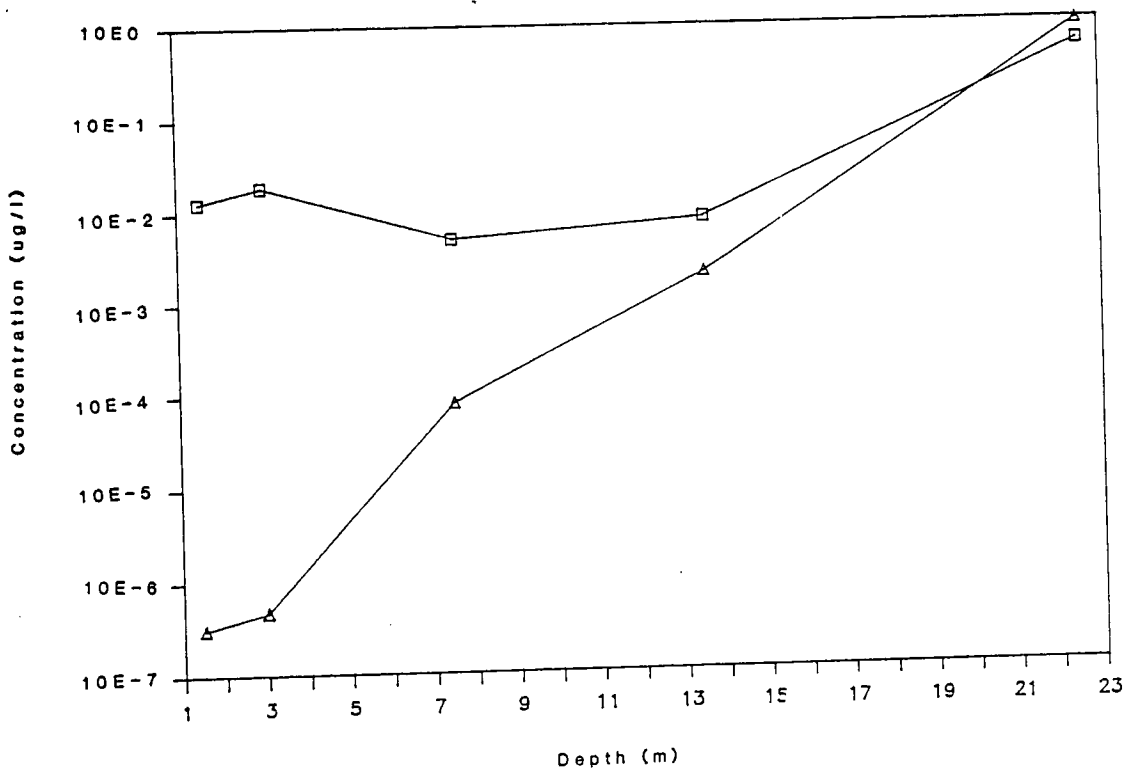


Figure 4.8 Concentration profile of scenario 6b, triangles, after 25 years and the measured concentration profile, squares.

TABLE 4.11

TCE Concentration ($\mu\text{g/l}$) profile of scenario 7 after 25 years and the measured concentration profile.

Depth (m)	Row No.	Concentration ($\mu\text{g/l}$)		Measured ($\mu\text{g/l}$)
		Without Advection	With Advection	
1.5	1	4.6 E-3	5.4 E-3	1.3 E-2
3.0	2	6.1 E-3	8.2 E-2	1.9 E-2
7.5	5	9.9 E-3	2.2 E-2	5.0 E-3
13.5	9	3.3 E-2	6.8 E-2	8.0 E-3
22.5	15	6.8 E-1	1.7	5.8 E-1

The simulated concentrations with and without advection caused by barometric pressure fluctuations are of the same order of magnitude as the measured concentration profile. The addition of advective transport increased the concentrations at every station, but not greatly, and also changed the shape of the concentration profile from monotonic to nonmonotonic. When there was a bypass mechanism around restrictive layers, as in scenario 3, the increase in concentrations when advective transport, caused by barometric pressure fluctuations, was included, was not as significant as when there was a horizontally homogeneous, layered system as in scenario 6. Hence, the effect of a advective transport was minor compared with the effect of a by-pass mechanism for TCE diffusional transport.

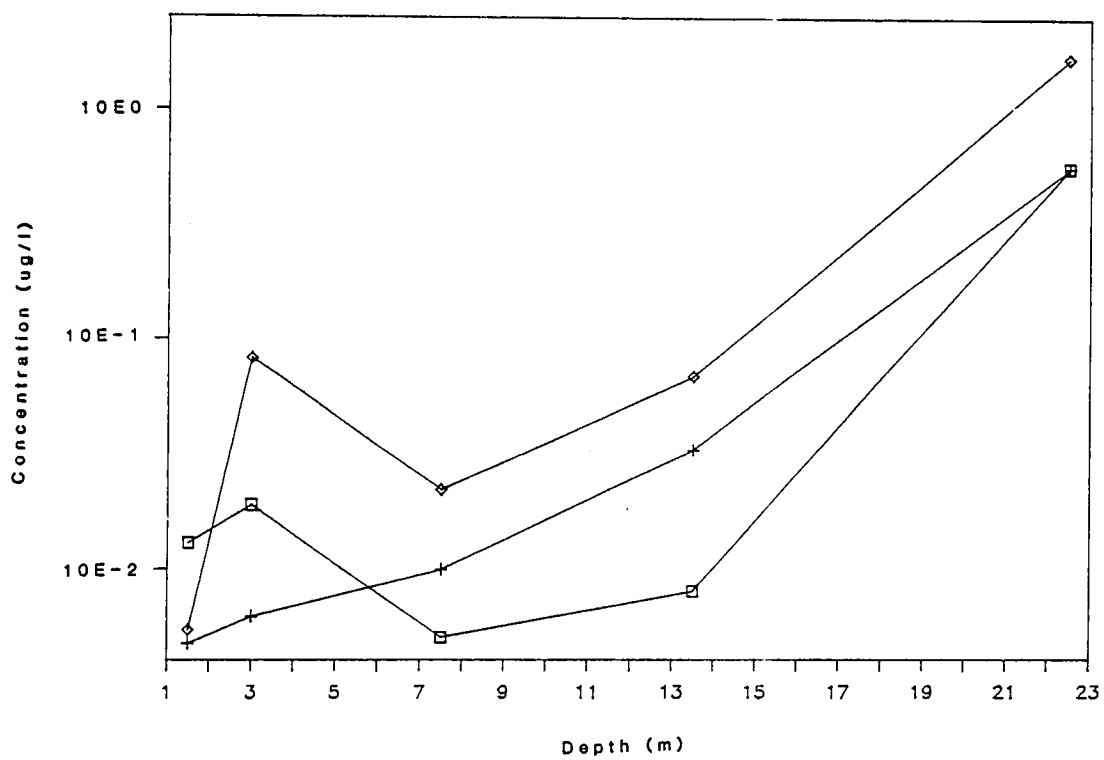


Figure 4.9 Concentration profile of scenario 7 after 25 years. Without advection, plus sign, with advection, diamonds, and the measured concentrations, squares.

CHAPTER 5

SUMMARY AND CONCLUSIONS

Past disposal practices of Trichloroethylene (TCE) and other halogenated hydrocarbons have resulted in the contamination of groundwater in part of the Tucson Basin. At the Carranza site, known to overlie a TCE groundwater contamination plume, a nest of gas sampling piezometers were constructed to measure the vertical distribution of TCE vapor in the vadose zone. The measured distribution of TCE vapor in the vadose zone was nonmonotonically decreasing from the water table to the atmosphere. This result was unexpected as the groundwater was postulated as the only source and the atmosphere as an infinite sink.

To investigate the nonmonotonic TCE concentration profile simulation studies were undertaken to test various hypotheses concerning the transport mechanisms of TCE vapor in the vadose zone. Transport of TCE vapor by gaseous diffusion and diurnal barometric pressure fluctuations were studied. An air/water/soil distribution coefficient was used in the computer simulations. Properties of the porous medium such as water content, degree of saturation, grain size distribution, and porosity were incorporated into the computer simulations.

The computer model used to investigate the TCE concentration profile measured at the Carranza site was the Discrete-State Compartment (DSC) model. The DSC model is solved by iteration of a recursive mass-

balance equation. The DSC model is flexible because the hydrologic system being modeled is discretized into a network of interconnected compartments that can vary in all physical parameters, including porosity, air porosity, water content, and distribution coefficients. The network of compartments can be arranged in 1-, 2-, or 3-dimensional arrays. Inputs to and outputs from the model can be made from any compartment and can vary with time. Radioactive decay, first-order chemical reactions, and age distribution are included in the DSC model. The DSC model is programmed for use on a personal computer which saves time and money because use of a mainframe computer is not needed.

The DSC computer code was shown to accurately reproduce the effects of diffusion through a homogeneous system with constant boundary conditions and a uniform initial concentration when compared to an analytical solution of Fick's second law.

The simulation studies tested various hypotheses concerning the transport mechanisms of TCE vapor in the vadose zone. All possible mechanisms were not tested. Conclusions based on the simulation studies were reached using only the data available at the Carranza site.

The simulation studies were divided into seven separate scenarios. Scenario 1a, was based on the following assumptions: (1) The vadose zone was homogeneous, (2) the mechanism of TCE transport was molecular diffusion, (3) diffusion was only in the vertical direction, (4) the base of the zone (interface with water table) received a constant source (input), (5) the top of the zone (interface with the atmosphere) was an infinite sink, and (6) TCE did not sorb with the liquid or solid phases of the vadose zone. An effective diffusion coefficient, D_e , was chosen

such that the concentration near the base of the model, after 25 years, equaled the measured concentration at the same depth. For scenario 1a, $D_a = 3.63 \text{ E-3 m}^2/\text{day}$. This was orders of magnitude larger than 14 of the 18 apparent diffusion coefficients calculated for the Carranza site.

Scenario 1b was based on the same assumptions as 1a, except that the interface with the water table received a variable source. An arbitrary source of TCE of 16.0 ug/l, from 0 to 5 years, 1600 ug/l, from 5 to 10 years, and 16.0 ug/l, from 10 to 25 years, was used. The variable source of TCE was found to create a nonmonotonic concentration profile.

Scenario 2 was based on the following assumptions: (1) The vadose zone was homogenous in the horizontal direction but nonhomogenous in the vertical direction. Heterogeneities were accounted for in the model by changing the values of the apparent diffusion coefficient. (2) the mechanism of TCE transport was molecular diffusion, (3) diffusion was only in the vertical direction, (4) the base of the zone (interface with water table) received a constant source (input), (5) the top of the zone (interface with the atmosphere) was an infinite sink, and (6) TCE sorbed instantaneously with the liquid and solid phases of the vadose zone.

Scenario 2 was also 1-dimensional. A time step of one week was used for a total time length of 25 years. Simulated concentrations in scenario 2 at the four shallowest sampling stations were many orders of magnitude lower than the concentration profile measured at the Carranza site. Evidently, layers of clay or silty-clay greatly restricted the rate of diffusion.

Scenario 3 was based on the same six assumptions as scenario 2, except that a high permeable column (HPC) was assumed to exist. Hence,

this scenario was a 2-dimensional system. The apparent diffusion coefficient of the HPC was $2.00 \text{ E-}2$. The addition of the HPC resulted in concentrations that were of the same order of magnitude as the measured concentrations.

In scenario 4 horizontal heterogeneities were added to the compartmental system of scenario 3. With this addition the simulated concentrations closely matched the measured concentrations.

Scenario 5 was based on the same assumptions as scenario 2, except that additional sources of TCE were included at intermediate depths above the water table. Lacking field data, the gradients chosen for the horizontal sources were arbitrary. With these additional sources in the vadose zone the measured concentration profile was closely simulated.

Scenario 6 was based on the same assumptions as scenario 2, except that cyclic vertical advection of soil gas, caused by diurnal barometric fluctuations, was superimposed on diffusion from the water table. The system was 1-dimensional. A time step of 12 hours was used for a total time length of 25 years. With the addition of advection of soil gas the simulated concentrations at 13.5 m and 22.5 m were of the same order of magnitude as the measured concentrations. At 1.5 m, 3.0 m, and 7.5 m the simulated concentrations were several orders of magnitude smaller than the measured concentrations.

Scenario 7 was based on the same assumptions as scenario 3, except that cyclic vertical advection of soil gas, caused by diurnal barometric fluctuations, was superimposed on diffusion from the water table. This

resulted in only a small increase in the simulated concentrations of scenario 2.

Undoubtedly, other hypotheses and scenarios could have been proposed and tested. This report provides a sampling of what might be done based on the limited amount of available field data.

Several conclusions can be drawn from the results of the seven scenarios concerning the distribution of TCE in the vadose zone. The vertical distribution of TCE in the vadose zone is controlled by more than vertical gaseous diffusion. The stratigraphy of the vadose zone is important. Vertical and horizontal heterogeneities can profoundly influence the mass transport by diffusion. The stratigraphy of the vadose zone will also affect the distribution of water in the vadose zone. A increase of the soil water content will decrease the air porosity which will decrease the effective diffusion coefficient. Horizontal fluxes of TCE could be produced by stratigraphic units of small effective diffusion coefficients next to units of larger effective diffusion coefficients.

Barometric pressure fluctuations have an affect on the TCE distribution in the vadose zone. The effect of barometric pressure fluctuations may or may not be signifcant depending on the parameters of the vadose zone; stratigraphy, soil-water distribution, air porosity.

Sources of TCE located in the vadose zone can change the nature of the concentration profile form a monotonic to a nonmonotonic concentration profile.

Variable sources at the water table can produce nonmonotonic TCE concentration profiles. In a homogenous system these concentration profiles are not similar in shape to the measured TCE concentration profile.

If shallow soil-gas sampling is to be used to delineate contaminated groundwater plumes the movement of volatile organic compounds in the vadose zone and the parameters affecting their movement must be understood. These parameters include vadose zone heterogeneities, soil/water- and gas/soil-distribution coefficient, air porosity, grain size distribution, recharge zones, climatic effects, and the proximity of the original disposal area to the sampling location. The use of shallow soil-gas sampling is an important remote sensing technique of contamination in the groundwater and vadose zone but direct correlation between near surface concentrations with groundwater concentrations should not be assumed because of the complicated interconnections between the parameters of the vadose zone and the TCE distribution in the vadose zone.

**Page Missing
in Original
Volume**

**Page Missing
in Original
Volume**

**Page Missing
in Original
Volume**

REFERENCES

- Campana, M. E., 1975. Finite State Models of Transport Phenomena in Hydrologic Studies. Dissertation, University of Arizona, Tucson, Arizona.
- Crank, J., 1975. The Mathematics of Diffusion, 2nd ed., Clarendon Press, Oxford, England.
- Dyksen, J. E., and A. F. Hess, 1982. Alternatives for controlling organics in groundwater supplies. J. Am. Water Works Assoc., V. 74, pp. 394 - 403.
- Freeze, R. A., and J. A. Cherry, 1979. Groundwater, Prentice-Hall, Inc. Englewood Cliffs, New Jersey.
- Hargis an Montgomery, Inc., 1982. Phase 1 investigations of subsurface conditions in the vicinity of abandoned waste disposal sites, Hughes Aircraft Company, Tucson, Arizona. Prepared for Latham and Watkins, San Diego, California.
- Hillel, D., 1972. Physiological Ecology, Academic Press, New York, New York.
- Hillel, D., 1980. Fundamentals of Soil Physics, Academic Press, New York, New York.
- Himmelblau, D. M., and K. B. Bischoff, 1968. Process Analysis and Simulation: Deterministic Systems, John Wiley and Sons, Inc.

- Kreamer, D. K., R. F. Bandeen, R. H. Seidemann, and M. E. Roberts, 1984. Support Material For the Tracer Technology Document. Report for Reynolds Electrical and Engineering Company , Las Vegas, Nevada.
- Kreamer, D. K., G. M. Thompson, E. S. Simpson, K. Stetzenback, and A. Long, 1985. Seasonal, Diurnal, and Storm Related Changes in Concentrations of Trichloroethzlene (TCE) and other Volatile Organics in the Unsaturated Zone. Completion report for Water Resources Research Center, Tucson, Arizona.
- Lyman, W. J., W. F. Reehl, and D. H. Rosenblatt, 1982. Handbook of Chemical Physical Estimation Methods, McGraw-Hill Book Co., New York.
- Marrin, D. L., 1984. Remote Detection and Preliminary Hazard Evaluation of Volatile Organic Contaminants in Groundwater, Dissertation, University of Arizona, Tucson, Arizona.
- Millington, R. J., 1959, Gas diffusion in porous media, Science, v. 130, p. 100 - 102.
- James M. Montgomery, Inc., and Johnson - Brittain and Assoc., Inc., 1984. Tucson Water Treatment Plant Project, Phase 1: Preliminary Investgations. Prepared for the Tucson Water Dept., Tucson, Arizona.
- Osborn, M. D., 1987. Modeling Nitrates in, Projecting the Future Ground-Water Quality of the Cortaro Area, Arizona, Thesis, University of Arizona, Tuscon, Arizona.
- Rasmussen, T. C., 1982. Solute Transport in Saturated Fractured Media, Thesis, Universtiy of Arizona, Tucson, Arizona.
- Roberts, M., 1986. The Use of Fluorocarbon Tracers to Monitor the Movement of Water in Unsaturated Porous Media: Column Study and Computer Model, Thesis, Universtiy of Arizona, Tucson, Arizona.

- Samper - Calvete, F. J., E. S. Simpson, and M. R. Llamas, 1985. New Developments in Groundwater Dating using Discrete-State Compartment Models.
- Slattery, J. C., and R. B. Bird, 1958. Calculation of the diffusion coefficient of dilute gases and of the self-diffusion coefficient of dense gases, *Am. Inst. Chem. Eng. J.*, v. 4(2), p. 137-142.
- Thomson, K. A., 1985. Vertical Diffusion of Selected Volatile Organic Contaminants Through Unsaturated Soil From a Water Table Aquifer; Field and Laboratory Studies. Thesis, University of Arizona, Tucson, Arizona.
- Turin, J., 1986. Carbon Dioxide and Oxygen Profiles in the Unsaturated Zone of the Tucson Basin, M.S. Prepublication Manuscript, University of Arizona, Tucson, Arizona.
- Weeks, E. P. 1978. Field determination of vertical permeability to air in the unsaturated zone. Open-File Report 77-346, U.S. Geol. Survey, Professional Paper 1051, Department of Interior.
- Weeks, E. P., D. E. Earp, and G. M. Thompson, 1982. Use of atmospheric fluorocarbons F-11 and F-12 to determine the diffusion parameters of the unsaturated zone in the Southern High Plains of Texas. *Water Res. Res.*, V.18, no.5.